deparaffinized, autoclaved at 121 °C for 5 min, and then immersed into 3% (v/v) H_2O_2 solution diluted in methanol for 10 min at room temperature to block endogenous peroxidase. Thereafter the sections were incubated in a solution containing primary antibody at 37 °C for 60 min followed by incubation with secondary antibodies at 37 °C for 30 min. In order to visualize the protein-antibody complexes, the sections were treated with Envision polymer reagent (DAKO, Tokyo, Japan) at 37 °C for 30 min, followed by treatment with 3,3′-diaminobenzidine tetrahydrochloride. The sections were counter-stained with Mayer's haematoxylin.

2.8. Statistical analysis

Data are expressed as means ± standard error of the mean (S. E. M.). Statistical comparisons among group mean values were performed by Kruskal–Wallis test or ANOVA followed by the Tukey test or Student's *t*-test. Significant difference was accepted at $P<0.05$.

3. Results

3.1. Time course of the change in GRP78 expression after renal ischemia-reperfusion

First, we ascertained a pattern of renal function after ischemia-reperfusion in the mice used in this study. As shown in Fig. 1, plasma urea nitrogen and creatinine concentrations gradually increased, reaching a peak at 48 h after ischemia-reperfusion for urea nitrogen and at 24 h for creatinine, and then decayed.

Next, we examined the time course of expression of the mRNAs for XBP-1s and GRP78, both of which are unfolded protein response targets (Schröder and Kaufman, 2005; Feldman et al., 2005; Xu et al., 2005), using RNA extracted from whole kidney. Fig. 2A shows representative photographs of the RT-PCR experiments and Fig. 2B and C summarize the quantified data. XBP-1s mRNA was clearly up-regulated at 1 h and 2 h after ischemia-reperfusion. This was followed by up-regulation of GRP78 mRNA, which reached a peak at 6 h after ischemia-reperfusion.

We then determined the expression level of GRP78 protein. Protein was extracted from mouse whole kidney and the extracted protein was subjected to immunoblotting. Fig. 2D shows representative blots and Fig. 2E summarizes the quantified data. GRP78 protein was increased at 6 h and 24 h and then decreased to the original level. These data clearly indicate that ischemia-reperfusion activated the unfolded protein response and that this activation preceded the peak of the renal function deficit.

3.2. Distribution of GRP78 in kidney after renal ischemia-reperfusion

The distribution of GRP78 protein was elucidated by immunohistochemistry. As shown in Fig. 3A, slight staining with anti-GRP78 antibody was observed in kidneys from mice subjected to sham operation. In contrast, ischemia-reperfusion produced widespread strong staining with anti-GRP78 antibody in the kidney, especially in the cortico-medullary boundary area (Fig. 3B). At higher magnification (Fig. 3C), the GRP78 protein induced by ischemia-reperfusion could be seen to be mainly distributed in proximal tubular cells. In the proximal tubular cells, GRP78 was located intracellularly.

3.3. Effect of tunicamycin on unfolded protein response targets

Mice were treated with tunicamycin, which is well known to act as an unfolded protein response inducer via inhibition of glycosylation (Price and Calderwood, 1992; Kaufman, 1999), and the expression of unfolded protein response targets was examined. The mice were divided into two groups. The control group was treated with vehicle and the experimental group was treated with 1.5 mg/kg tunicamycin.

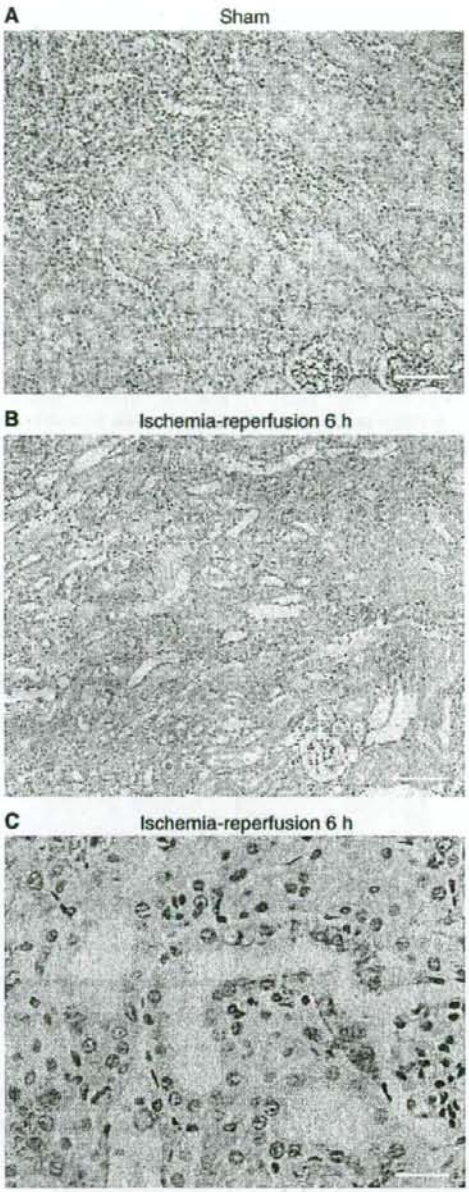

Fig. 3. Immunohistology for GRP78 protein in kidney after renal ischemia-reperfusion. Kidneys were removed 6 h after sham or renal ischemia-reperfusion operation, and were fixed in 10% formaldehyde solution, embedded in paraffin, and then sectioned for immunohistochemical staining with polyclonal rabbit anti-GRP78 antibody. (A) Representative staining in kidney from a mouse subjected to sham operation at low magnification. (B, C) Representative staining in kidney from a mouse subjected to ischemia-reperfusion operation are shown at low (B) and high (C) magnification. Brown staining indicates the presence of GRP78. No brown staining was observed if the primary antibody was omitted (control staining). Scale bars = 100 μm in A and B, 25 μm in C.

Kidney samples were obtained 48 h after the treatments. As shown in Fig. 4A, tunicamycin clearly increased the expression of XBP-1s and GRP78 mRNA. Furthermore, tunicamycin also increased protein

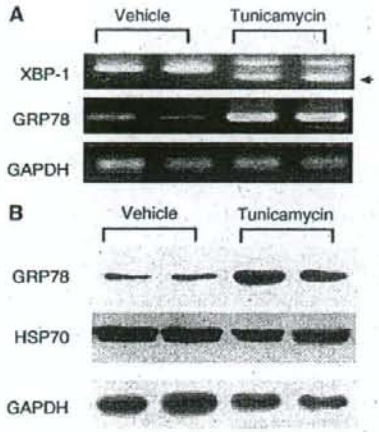

Fig. 4. Effect of treatment with tunicamycin on the expression levels of XBP-1s and GRP78 mRNA, and GRP78 protein. Kidneys were removed 48 h after treatment with vehicle or tunicamycin and then total RNA and protein were extracted. (A) A splicing form of XBP-1 (arrow head), GRP78, and GAPDH mRNA were determined by RT-PCR analysis. (B) GRP78, HSP70 and GAPDH (internal control) protein was detected by Western blot.

expression of GRP78 (Fig. 4B). In contrast, tunicamycin had no effect on the expression level of HSP70, a member of the same protein family as GRP78 (Fig. 4B). Fig. 5 shows the renal distributions of GRP78 after treatment with tunicamycin. Without tunicamycin-treatment, expression of GRP78 was weak (Fig. 5A). After tunicamycin treatment, GRP78 expression markedly increased in the renal cortex and corticomedullary boundary area (Fig. 5B). Higher magnification (Fig. 5C) clearly showed that the GRP78 induced by treatment with tunicamycin was mainly distributed in the cytoplasm of proximal tubular cells. In contrast to the up-regulation of GRP78 immunohistochemical analysis also exhibited that no enhanced expression of HSP70 was observed by treatment with tunicamycin (data not shown), confirming the immunoblotting data. These results clearly show that treatment with tunicamyin specifically induced the unfolded protein response in proximal tubular cells.

We next studied the effect of thapsigargin, which is also known to be an unfolded protein response inducer like tunicamycin (Price and Calderwood, 1992; Kaufman, 1999; Kondoh et al., 2004), on renal GRP78 expression. Kidney samples were obtained 24 h after treatment with thapsigargin. Immunohistochemical analysis showed that thapsigargin up-regulated protein expression of GRP78 in the same renal areas as did tunicamycin (data not shown). In contrast to this, increased expression of HSP70 was not observed by treatment with thapsigargin (data not shown), indicating specific activation of the unfolded protein response by thapsigargin.

3.4. Effect of tunicamycin treatment on ischemia-reperfusion injury

Next, we studied the effect of tunicamycin on renal ischemia-reperfusion injury. Mice were treated with vehicle (control group) or tunicamycin (1.5 mg/kg) 2 days prior to ischemia-reperfusion and kidney samples were obtained 24 h after ischemia-reperfusion. Fig. 6 shows the results of histopathological analysis (PAS staining) and plasma creatinine concentration. Histopathological analysis with PAS staining revealed that ischemia-reperfusion caused cast formation in tubules, tubule dilatation, and epithelial cell death in the cortex and outer medulla (Fig. 6A). Tunicamycin ameliorated these pathological changes (Fig. 6B). Semi-quantitative measurement of the PAS-positive area showed that this was significantly smaller in the tunicamycin group than that in the controls (Fig. 6C). In accordance with the histopathological results, the plasma concentration of creatinine in the tunicamycin group was significantly lower than that in the control group at 24 h after ischemia-reperfusion (Fig. 6D).

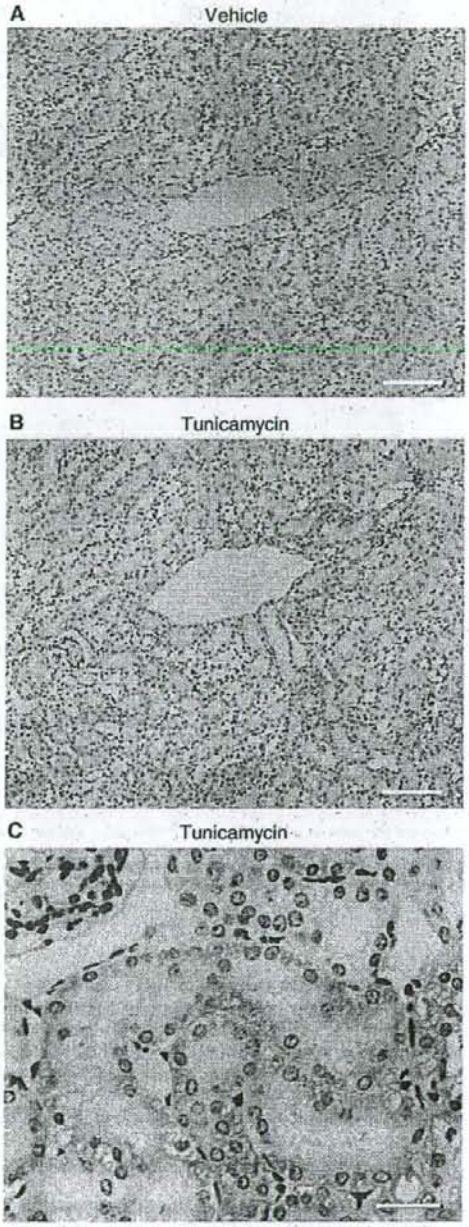

Fig. 5. Immunohistology for GRP78 protein in kidney after treatment with tunicamycin. Kidneys were removed 48 h after treatment with vehicle (PBS) or tunicamycin (1.5 mg/kg). Representative staining for GRP78 protein in kidney after treatment with vehicle at low magnification (A) or with tunicamycin at low (B) and high (C) magnification are shown. Scale bars = 100 μm in A and B, 25 μm in C.

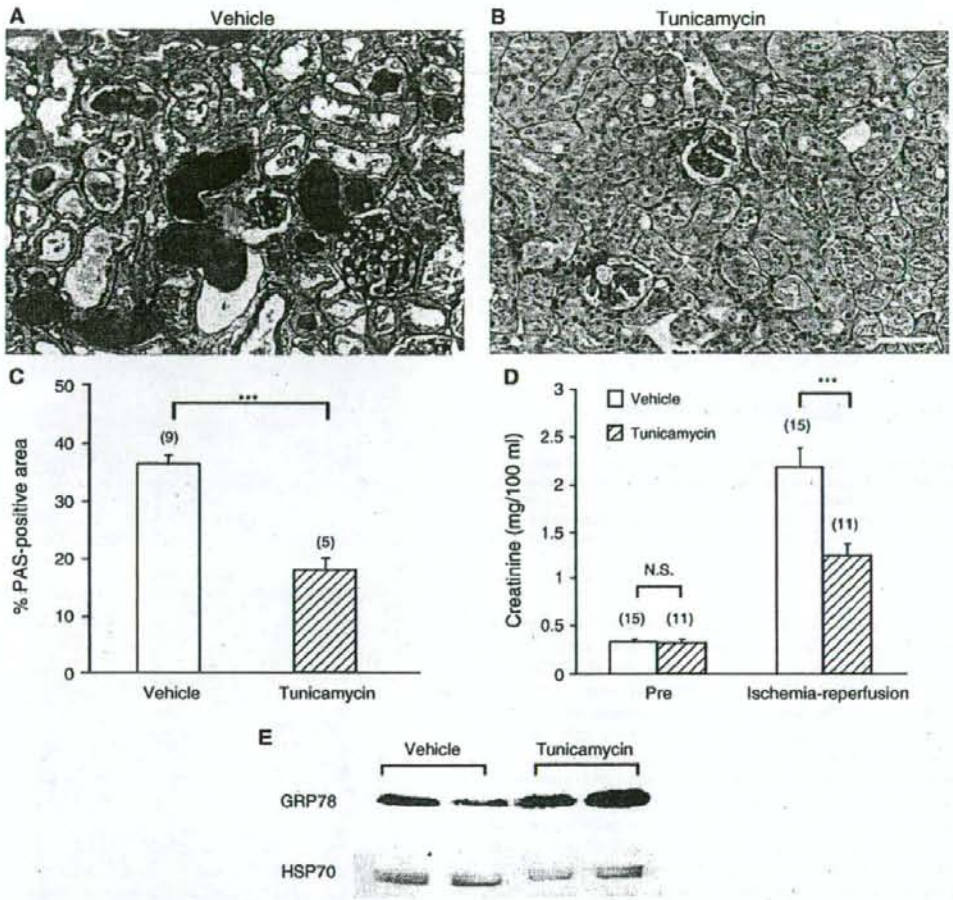

Fig. 6. Effect of tunicamycin on renal ischemia-reperfusion injury. Tunicamycin (1.5 mg/kg) or vehicle (PBS) was administered to mice 48 h before ischemia-reperfusion operation. (A, B, C) PAS staining was performed on kidney sections obtained 24 h after ischemia-reperfusion from mice treated with vehicle (A) or tunicamycin (B). The renal cortex and cortico-medullary junction were shown. A scale bar=50 μm. The PAS-positive-area was measured as described in Materials and methods (C). Values are means±S. E. M. Numbers in parentheses are the numbers of animals tested. ***$P<0.001$; significantly different from the value of vehicle-treatment group. (D) Plasma for measurement of creatinine concentration was collected before (Pre) and 24 h after ischemia-reperfusion. Values are means±S. E. M. Numbers in parentheses are the numbers of animals tested. ***$P<0.001$; significantly different from the value of vehicle-treatment group. N.S.; not significantly different from the value of vehicle-treatment group. (E) Representative blots for GRP78 and HSP70. Kidneys treated with vehicle or tunicamysin were removed 24 h after ischemia-reperfusion and protein was extracted.

When we compared the expression level of GRP78 between the control and tunicamycin groups by immunoblotting after renal ischemia-reperfusion, GRP78 expression was clearly higher in the tunicamycin group (Fig. 6E). In contrast, the level of HSP70 expression did not differ between the groups. These data clearly show that treatment of mice with tunicamycin attenuated ischemia-reperfusion injury with concomitant enhancement of renal GRP78 expression.

3.5. Effect of thapsigargin treatment on ischemia-reperfusion injury

Mice were treated with vehicle (control group) or with thapsigargin (1 mg/kg). Fig. 7 shows the results of histopathological analysis and plasma creatinine concentration. Treatment with thapsigargin ameliorated renal function and injury after renal ischemia-reperfusion. As seen in Fig. 7C and D, treatment with the vehicle for thapsigargin (DMSO) tended to reduce the severity of renal injury in comparison with the vehicle for tunicamycin (Fig. 6C and D). Since DMSO is known to be an antioxidant, and reactive oxygen species have been reported to worsen renal ischemia-reperfusion injury, this reduction may be explained by the antioxidant effect of DMSO.

4. Discussion

Several *in vitro* studies with cultured tubular cells have examined the unfolded protein response activation in response to renal ischemia-reperfusion and its role against cell injury using chemical unfolded protein response inducers. In a proteomic study, Kumar et al. (2003) reported that simulated ischemia-reperfusion in cultured tubular LLC-PK1 cells increased GRP78 and HSPs. In Madin–Darby canine kidney cells (Bush et al., 1999; George et al., 2004), ATP depletion by treatment with antimycin, followed by recovery in medium without antimycin, resulted in up-regulation of GRP78. This

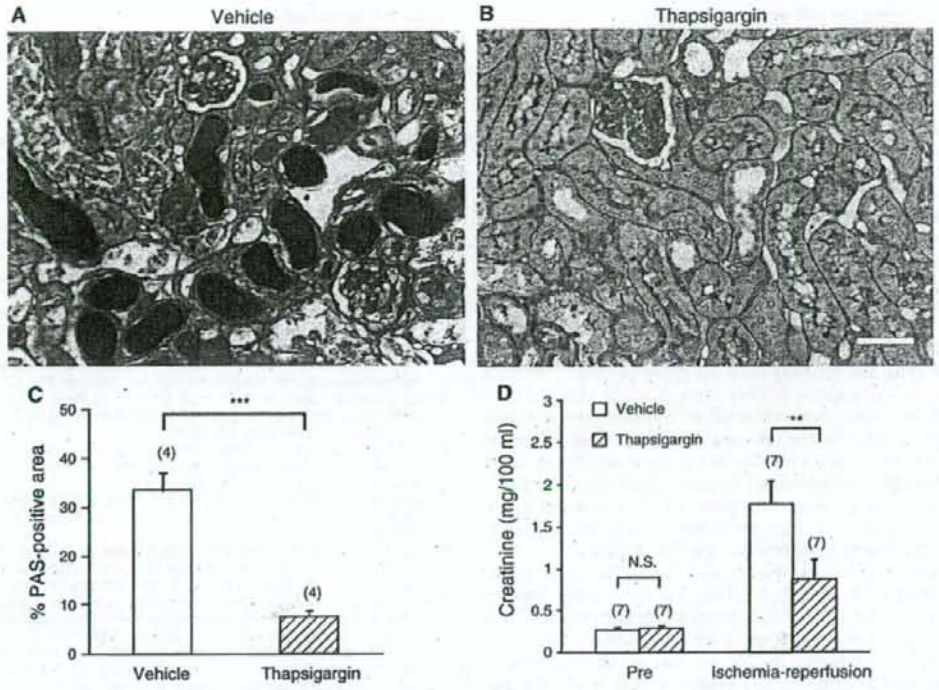

Fig. 7. Effect of thapsigargin on renal ischemia-reperfusion injury. Thapsigargin (1 mg/kg) or vehicle (DMSO) was administered to mice 24 h before ischemia-reperfusion operation. (A, B, C) PAS staining was performed on kidney sections obtained 24 h after ischemia-reperfusion from mice treated with vehicle (A) or thapsigargin (B). The renal cortex and cortico-medullary junction were shown. A scale bar=50 μm. The PAS-positive-area was measured (C). Values are means±S. E. M. Numbers in parentheses are the numbers of animals tested. ***$P<0.001$; significantly different from the value of vehicle-treatment group. (D) Plasma for measurement of creatinine concentration was collected before (Pre) and 24 h after ischemia-reperfusion. Values are means±S. E. M. Numbers in parentheses are the numbers of animals tested. **$P<0.01$; significantly different from the value of vehicle-treatment group. N.S.; not significantly different from the value of vehicle-treatment group.

up-regulation was accompanied by cell injury, and pretreatment of the cells with tunicamycin protected against antimycin-induced cell injury with an enhancement of the expression of GRP78. Nevertheless, although some *in vivo* studies have shown up-regulation of unfolded protein response-related proteins such as GRP78 (Kuznetsov et al., 1996), GRP94 (Kuznetsov et al., 1996), an autophosphorylated form of PERK (Montie et al., 2005), a phosphorylated form of eIF2α (Montie et al., 2005), the 150 kDa oxygen-regulated protein (Bando et al., 2004), and ER protein 72 (Kuznetsov et al., 1996) in mouse kidney after ischemia-reperfusion, the role of activation of the unfolded protein response in renal ischemia-reperfusion injury *in vivo* remains largely unknown. In the present study, we clearly showed that ischemia-reperfusion caused up-regulation of GRP78. This GRP78 was mainly distributed in the cortico-medullary boundary area, especially in the interior of proximal tubular cells, which is known to be susceptible to renal ischemia-reperfusion injury. Up-regulation of the chemical unfolded protein response was apparent at 6 h after ischemia-reperfusion, and this response subsequently returned to its original level within 24 h. Treatement with tunicamycin, known to be a specific chemical unfolded protein response inducer, clearly induced GRP78 expression mainly in the cortico-medullary boundary area. Pretreatment of mice with tunicamycin protected tubule cells from renal ischemia-reperfusion injury with enhancement of GRP78 protein expression. Thapsigargin, another inducer of chemical unfolded protein response, mimicked the effect of tunicamycin. Taken together with the earlier *in vitro* data, these observations provide strong evidence that the unfolded protein response is activated in the renal sites that are susceptible to ischemia-reperfusion injury, and that this activation is involved in protection against this type of injury. To our knowledge, this is the first study to have demonstrated a protective effect of chemical unfolded protein response inducers against renal ischemia-reperfusion injury *in vivo*.

We observed strong expression of GRP78 at the cortico medullary junction in response to ischemia-reperfusion. A phosphorylated form of eIF2α has been reported to be localized in the same region after renal ischemia-reperfusion (Montie et al., 2005). These data indicate that activation of the unfolded protein response occurs predominantly in this region, which is known to be poorly vascularized (Montie et al., 2005) and susceptible to renal ischemia-reperfusion. In addition, Yin et al. (2002) observed a dramatic increase of hypoxia at the cortico-medullary junction 24 h after renal ischemia-reperfusion relative to that in the cortex and inner medulla. Therefore, the selective induction of GRP78 in this area may be a reflection of the severity of hypoxia following ischemia-reperfusion.

Administration of tunicamycin to mice causes renal tubular cell apoptosis through activation of the unfolded protein response. Ron and colleagues examined the role of the C/EBP homologous protein-10 (CHOP), also known as GADD153, which is a molecule downstream from PERK, in *chop* −/− mice treated with tunicamycin (Zinszner et al., 1998; Marciniak et al., 2004). They showed that tunicamycin induced conspicuous renal tubule cell apoptosis in the juxtamedullary region of wild-type mice and that this apoptosis was reduced in *chop* −/− mice, suggesting that tunicamycin-induced renal epithelial apoptosis is partly mediated by the PERK-CHOP pathway. Using mice, Nakagawa

et al. (2000) studied the involvement of caspase-12, an endoplasmic reticulum stress-related, in renal tubule epithelial cell death after tunicamycin treatment. Wild-type mice injected with tunicamycin showed a significant number of TUNEL-positive (DNA-fragmented) renal epithelial cells, whereas fewer TUNEL-positive cells were found in *caspase-12 −/−* kidney. This also suggests that tunicamycin causes epithelial cell apoptosis via activation of the unfolded protein response and therefore that treatment with tunicamycin alone might cause renal injury. However, in the present study treatment with tunicamycin alone had no effect on renal function (Fig. 6D), and moreover had a protective effect against renal ischemia-reperfusion injury. Similar findings have also been obtained by several other groups (Zinszner et al., 1998; Takano et al., 2007). It is currently unclear why tunicamycin can either ameliorate renal ischemia-reperfusion injury or cause apoptosis, but one possible explanation is a dual effect of unfolded protein response activation, which may lead to differential susceptibility of tubule epithelial cells via either a pro-survival or a pro-apoptotic phenotype. A minor population of renal tubule epithelial cells subjected to more intense unfolded protein response activation by tunicamycin might undergo apoptotic cell death, whereas a larger number of less intensely affected renal tubule cells might suffer inhibition of protein synthesis that is caused by unfolded protein response activation, which is followed by an increase in the processing capacity of the endoplasmic reticulum, leading to cell recovery from ischemia-reperfusion injury.

HSP70 belongs to the same protein family as GRP78 (Benjamin and McMillan, 1998). It has been reported that HSP70 is up-regulated by ischemia-reperfusion and that this up-regulation leads to protection against renal ischemia-reperfusion injury (Suzuki et al., 2005). We therefore examined whether HSP70 was involved in protection by chemical unfolded protein response inducers against renal ischemia-reperfusion injury. None of the inducers such as tunicamycin and thapsigargin affected the expression of HSP70, suggesting that the unfolded protein response inducers used in this study exerted their effects independently of HSP70. Furthermore, we determined the expression level of HSC70, which is also a member of the HSP70 protein family (Benjamin and McMillan, 1998), and again found that expression of HSC70 was not affected by chemical unfolded protein response inducers (data not shown). These observations support the specificity of the chemical unfolded protein response inducers used in this study.

In the response to ischemia-reperfusion, up-regulation of XBP-1s transcript clearly preceded that of GRP78 transcript. Since transactivation of the gene by XBP-1s has been shown to be dependent on a sequence present in the GRP78 promoter, this strongly suggests that XBP-1s functions as a transcription factor for GRP78. In fact, the level of GRP78 mRNA has been reported to be constitutively elevated in cells overproducing XBP-1 (Yoshida et al., 2001). However, Lee et al. (2003) showed that the induction of GRP78 by tunicamycin was only modestly dependent on XBP-1 in XBP-1-deficient mouse embryo fibroblast cells as well as in XBP-1/ATF6α doubly deficient mouse embryo fibroblast cells, and they concluded that there is an additional *cis*-acting element in addition to those for XBP-1s and ATF6 in the GRP78 promoter that is responsible for its endoplasmic reticulum-stress-induced expression. In contrast to this report, Thuerauf et al. (2006) recently investigated the functional role of XBP-1 in cultured cardiac myocytes infected with a recombinant adenovirus encoding dominant-negative XBP-1 and then subjected to tunicamycin and hypoxia/reoxygenation. They observed that GRP78 expression in response to treatment with tunicamycin and to hypoxia/reoxygenation depended on the expression level of XBP-1, and that expression of dominant-negative XBP-1 worsened hypoxia/reoxygenation-induced cell injury. Together, these reports suggest a cell-type-dependence for the regulation of GRP78 expression by XBP-1. The detailed molecular mechanisms by which renal ischemia-reperfusion up-regulates GRP78 await clarification in future studies.

Acknowledgements

This work was supported in part by JSPS KAKENHI, 19580342 (M.I.).

References

Bando, Y., Tsukamoto, Y., Katayama, T., Ozawa, K., Kitao, Y., Hori, O., Stern, D.M., Yamauchi, A., Ogawa, S., 2004. ORP150/HSP12A protects renal tubular epithelium from ischemia-induced cell death. FASEB J. 18, 1401–1403.

Benjamin, I.J., McMillan, D.R., 1998. Stress (heat shock) proteins: molecular chaperones in cardiovascular biology and disease. Circ. Res. 83, 117–132.

Bush, K.T., George, S.K., Zhang, P.L., Nigam, S.K., 1999. Pretreatment with inducers of ER molecular chaperones protects epithelial cells subjected to ATP depletion. Am. J. Physiol. Renal Physiol. 277, F211–F218.

Devarajan, P., 2006. Update on mechanisms of ischemic acute kidney injury. J. Am. Soc. Nephrol. 17, 1503–1520.

Feldman, D.E., Chauhan, V., Koong, A.C., 2005. The unfolded protein response: a novel component of the hypoxic stress response in tumors. Mol. Cancer Res. 3, 597–605.

George, S.K., Meyer, T.N., Abdeen, O., Bush, K.T., Nigam, S.K., 2004. Tunicamycin preserves intercellular junctions, cytoarchitecture, and cell-substratum interactions in ATP-depleted epithelial cells. Biochem. Biophys. Res. Commun. 322, 223–231.

Ikeda, M., Gunji, Y., Sonoda, H., Oshikawa, S., Shimono, M., Horie, A., Ito, K., Yamasaki, S., 2006a. Shiga toxin activates p38 MAP kinase through cellular Ca(2+) increase in Vero cells. Eur. J. Pharmacol. 546, 36–39.

Ikeda, M., Prachasilchai, W., Burne-Taney, M.J., Rabb, H., Yokota-Ikeda, N., 2006b. Ischemic acute tubular necrosis models and drug discovery: a focus on cellular inflammation. Drug Discov. Today 11, 364–370.

Kaufman, R.J., 1999. Stress signaling from the lumen of the endoplasmic reticulum: coordination of gene transcriptional and translational controls. Genes Dev. 13, 1211–1233.

Kondoh, M., Tsukada, M., Kuronaga, M., Higashimoto, M., Takiguchi, M., Himeno, S., Watanabe, Y., Sato, M., 2004. Induction of hepatic metallothionein synthesis by endoplasmic reticulum stress in mice. Toxicol. Lett. 148, 133–139.

Kumar, Y., Tatu, U., 2003. Stress protein flux during recovery from simulated ischemia: induced heat shock protein 70 confers cytoprotection by suppressing JNK activation and inhibiting apoptotic cell death. Proteomics 3, 513–526.

Kuznetsov, G., Bush, K.T., Zhang, P.L., Nigam, S.K., 1996. Perturbations in maturation of secretory proteins and their association with endoplasmic reticulum chaperones in a cell culture model for epithelial ischemia. Proc. Natl. Acad. Sci. U. S. A. 93, 8584–8589.

Lameire, N., Van Biesen, W., Vanholder, R., 2005. Acute renal failure. Lancet 365, 417–430.

Lee, A.H., Iwakoshi, N.N., Glimcher, L.H., 2003. XBP-1 regulates a subset of endoplasmic reticulum resident chaperone genes in the unfolded protein response. Mol. Cell. Biol. 23, 7448–7459.

Marciniak, S.J., Yun, C.Y., Oyadomari, S., Novoa, I., Zhang, Y., Jungreis, R., Nagata, K., Harding, H.P., Ron, D., 2004. CHOP induces death by promoting protein synthesis and oxidation in the stressed endoplasmic reticulum. Genes Dev. 18, 3066–3077.

Montie, H.L., Kayali, F., Haezebrouck, A.J., Rossi, N.F., Degracia, D.J., 2005. Renal ischemia and reperfusion activates the eIF 2 alpha kinase PERK. Biochim. Biophys. Acta 1741, 314–324.

Nakagawa, T., Zhu, H., Morishima, N., Li, E., Xu, J., Yankner, B.A., Yuan, J., 2000. Caspase-12 mediates endoplasmic-reticulum-specific apoptosis and cytotoxicity by amyloid-beta. Nature 403, 98–103.

Price, B.D., Calderwood, S.K., 1992. Gadd45 and Gadd153 messenger RNA levels are increased during hypoxia and after exposure of cells to agents which elevate the levels of the glucose-regulated proteins. Cancer Res. 52, 3814–3817.

Schröder, M., Kaufman, R.J., 2005. The mammalian unfolded protein response. Annu. Rev. Biochem. 74, 739–789.

Suzuki, S., Maruyama, S., Sato, W., Morita, Y., Sato, F., Miki, Y., Kato, S., Katsuno, M., Sobue, G., Yuzawa, Y., Matsuo, S., 2005. Geranylgeranylacetone ameliorates ischemic acute renal failure via induction of Hsp70. Kidney Int. 67, 2210–2220.

Takano, K., Tabata, Y., Kitao, Y., Murakami, R., Suzuki, H., Yamada, M., Iinuma, M., Yoneda, Y., Ogawa, S., Hori, O., 2007. Methoxyflavones protect cells against endoplasmic reticulum stress and neurotoxin. Am. J. Physiol., Cell Physiol. 292, C353–C361.

Thuerauf, D.J., Marcinko, M., Gude, N., Rubio, M., Sussman, M.A., Glembotski, C.C., 2006. Activation of the unfolded protein response in infarcted mouse heart and hypoxic cultured cardiac myocytes. Circ. Res. 99, 275–282.

Xu, C., Bailly-Maitre, B., Reed, J.C., 2005. Endoplasmic reticulum stress: cell life and death decisions. J. Clin. Invest. 115, 2656–2664.

Xue, J.L., Daniels, F., Star, R.A., Kimmel, P.L., Eggers, P.W., Molitoris, B.A., Himmelfarb, J., Collins, A.J., 2006. Incidence and mortality of acute renal failure in medicare beneficiaries, 1992 to 2001. J. Am. Soc. Nephrol. 17, 1135–1142.

Yin, M., Zhong, Z., Connor, H.D., 2002. Protective effect of glycine on renal injury induced by ischemia-reperfusion in vivo. Am. J. Physiol. Renal Physiol. 282, F417–F423.

Yokota, N., Daniels, F., Crosson, J., Rabb, H., 2002. Protective effect of T cell depletion in murine renal ischemia-reperfusion injury. Transplantation 74, 759–763.

Yoshida, H., Matsui, T., Yamamoto, A., Okada, T., Mori, K., 2001. XBP1 mRNA is induced by ATF6 and spliced by IRE1 in response to ER stress to produce a highly active transcription factor. Cell 107, 881–891.

Zinszner, H., Kuroda, M., Wang, X., Batchvarova, N., Lightfoot, R.T., Remotti, H., Stevens, J.L., Ron, D., 1998. CHOP is implicated in programmed cell death in response to impaired function of the endoplasmic reticulum. Genes Dev. 12, 982–995.

Neuroscience 151 (2008) 111–119

INVOLVEMENT OF ENDOPLASMIC RETICULUM STRESS IN THE NEURONAL DEATH INDUCED BY TRANSIENT FOREBRAIN ISCHEMIA IN GERBIL

Y. OIDA,[a] M. SHIMAZAWA,[a] K. IMAIZUMI[b] AND H. HARA[a]*

[a]*Department of Biofunctional Evaluation, Molecular Pharmacology, Gifu Pharmaceutical University, 5-6-1 Mitahora-higashi, Gifu 502-8585, Japan*

[b]*Division of Molecular and Cellular Biology, Department of Anatomy, Faculty of Medicine, University of Miyazaki, Kihara 5200, Kiyotake, Miyazaki 889-1692, Japan*

Abstract—Endoplasmic reticulum (ER) stress, which is caused by an accumulation of unfolded proteins in the ER lumen, is associated with stroke and with neurodegenerative diseases such as Parkinson's and Alzheimer diseases. We assessed the expression patterns of immunoglobulin heavy chain binding protein (BiP)/glucose-regulated protein (GRP) 78 (an ER-resident molecular chaperone whose expression serves as a good marker of ER-stress), activating transcription factor (ATF)-4, and C/EBP homology protein (CHOP) by immunohistochemistry and/or Western blotting after transient forebrain ischemia in gerbils. Double-fluorescent staining involving CHOP immunohistochemistry and the terminal deoxynucleotidyl transferase-mediated DNA nick-end labeling (TUNEL) method was performed to clarify the involvement of CHOP in cell death. Immunohistochemical and Western blot analyses of the hippocampal Cornet d'Ammon (CA)1 subfield showed that BiP expression was increased at 12 h, peaked at 3 days, then decreased (versus the control group). A transient increase was detected in CA3 at 1 day after ischemia, but BiP expression was unchanged in dentate gyrus and cortex. Signals for ATF-4 and CHOP were increased at 1 day and 3 days in CA1, and at 12 h in CA3. Co-localization of CHOP immunoreactivity and DNA fragmentation was detected by the TUNEL method at 3 days after ischemia in CA1, but not at 12 h in CA3. These findings are consistent with ER stress playing a pivotal role in post-ischemic neuronal death in the gerbil hippocampal CA1 subfield. **© 2008 IBRO. Published by Elsevier Ltd. All rights reserved.**

Key words: apoptosis, CHOP, ER-stress, BiP, ischemia, neuronal cell death.

*Corresponding author. Tel: +81-58-237-8596; fax: +81-58-237-8596.
E-mail address: hidehara@gifu-pu.ac.jp (H. Hara).

Abbreviations: ATF-4, activating transcription factor-4; BCA, bicinchoninic acid; BiP, immunoglobulin heavy chain binding protein; CA, Cornet d'Ammon; CHOP, C/EBP homology protein; CREB, cyclic AMP response element-binding protein; DAB, diaminobenzidine; DG, dentate gyrus; eIF2α, eukaryotic initiation factor 2α; ER, endoplasmic reticulum; GADD153, growth arrest and DNA damage-inducible gene; GFAP, glial fibrillary acidic protein; KDEL, COOH-terminal Lys-Asp-Glu-Leu; NeuN, neuronal nuclei; OASIS, old astrocyte specifically induced substance; PBS, phosphate buffered saline; PERK, RNA-dependent protein kinase-like endoplasmic reticulum eukaryotic initiation factor 2α kinase; RT-PCR, reverse-transcription polymerase chain reaction; TUNEL, terminal deoxynucleotidyl transferase-mediated DNA nick-end labeling.

0306-4522/08$32.00+0.00 © 2008 IBRO. Published by Elsevier Ltd. All rights reserved.
doi:10.1016/j.neuroscience.2007.10.047

Protein misfolding has been implicated in the pathogenesis of neurological diseases. For example, an accumulation of misfolded proteins, such as β-amyloid and α-synuclein, is apparently associated with the selective neuronal cell death that occurs in Alzheimer's and Parkinson's diseases, respectively. Moreover after focal brain ischemia and reperfusion, protein aggregation in the endoplasmic reticulum (ER) has been observed using electron microscopy analysis (Leroux et al., 2001). Recent studies have demonstrated that ER-stress is implicated in a variety of common diseases, such as diabetes, stroke, and neurodegenerative disorders. Various experimental models and observational studies have shown that cerebral ischemia induces an ER-stress response, suggesting that ER may play an important role in the pathogenesis of neuronal cell injury during and after cerebral ischemia (Ito et al., 2001; Mouw et al., 2003; Paschen et al., 2003; Morimoto et al., 2007). Most previous studies have employed middle cerebral artery occlusion (MCAO) models, not a transient global ischemia model.

In the ischemic focus of the infarcted brain of a patient who died after the onset of stroke, an expression of oxygen regulated protein (ORP) 150, which is an ER-associated chaperon, was detected in neurons and astrocytes, indicating that ER-stress may have been involved in the ischemic disturbance (Tamatani et al., 2001). However, the molecular mechanisms linked to ER-stress-mediated apoptosis and neuronal cell death remain to be studied.

Cells show a variety of responses when stress (such as glucose deprivation and hypoxia) is imposed on the ER. Together, protein synthesis inhibition and ER-resident molecular chaperone induction are known as the 'unfolded protein response' (Ma and Hendershot, 2001). These reactions can be seen as attempts to reduce the load on the ER and prevent a consequent cellular catastrophe. When the ER-stress is very severe, however, the affected cells activate the apoptotic machinery. In this process, proteins on the ER membrane are activated and dispatch cell-death signals to other parts of the cell (Nakagawa et al., 2000; Calfon et al., 2002). At least three apoptosis pathways are known to be involved in the apoptotic events related to ER-stress: 1) the transcriptional factor C/EBP homology protein (CHOP)/growth arrest and DNA damage-inducible gene (GADD153) –mediated pathway (Oyadomari and Mori, 2004), 2) the TNF receptor-associated factor 2 (TRAF2)–apoptosis signal-regulating kinase one (ASK1)–mediated pathway (Takeda et al., 2003), and 3) the caspase 12–mediated pathway (Nakagawa et al., 2000). In

the ischemic brain, RNA-dependent protein kinase-like endoplasmic reticulum eukaryotic initiation factor 2α (eIF2α) kinase (PERK) is activated (Kumar et al., 2001). This in turn phosphorylates eIF2α, which induces activating transcription factor-4 (ATF-4) (Harding et al., 2002). ATF-4 then induces CHOP, causing apoptosis (Harding et al., 2000, 2002). Hence, induction of ATF-4 and CHOP is the key step in ER stress-induced neuronal cell death after ischemia.

Against this background, we designed the present study to investigate the involvement of ER-stress in the execution of cell death in a transient forebrain ischemia model in the gerbil.

EXPERIMENTAL PROCEDURES

Experimental materials

Male adult Mongolian gerbils (Kyudo, Fukuoka, Japan), weighing 60–80 g, were used for experiments on transient global forebrain ischemia. The animals were allowed *ad libitum* access to food and water. The present experiments were performed in accordance with the Guidelines for Animal Experiments issued by Gifu Pharmaceutical University and the U.S. National Institutes of Health Guide for the Care and Use of Laboratory Animals. Attempts were made to limit the number, as well as pain and suffering, of animals used.

The drugs and materials used and their sources were as follows. Paraformaldehyde (Wako Pure Chemical Industries, Osaka, Japan), sucrose (Wako), sodium hydrogen phosphate 12-water (Nacalai tesque, Kyoto, Japan), sodium dihydrogen phosphate dihydrate (Nacalai tesque), potassium chloride (Wako), sodium chloride (Kishida Chemical, Osaka, Japan), nembutal (Dainippon Pharmaceutical, Osaka, Japan), Triton X-100 (Bio-Rad, Hercules, CA, USA), O.C.T. compound (Sakura Finetechnical, Tokyo, Japan), Vectastain elite ABC kit (Vector Laboratories, Burlingame, CA, USA), M.O.M. immunodetection kit (Vector Laboratories), diaminobenzidine (DAB) peroxidase substrate kit (Vector Laboratories), mouse anti-KDEL monoclonal antibody (Stressgen Bioreagents, Victoria, BC, Canada), mouse anti–immunoglobulin heavy chain binding protein (BiP) monoclonal antibody (Transduction Laboratories, Lexington, KY), mouse anti-neuronal nuclei (NeuN) monoclonal antibody (Chemicon, Temecula, CA, USA), mouse anti–glial fibrillary acidic protein (GFAP) monoclonal antibody (YLEM, San Francisco, CA, USA), rabbit anti-cyclic AMP response element-binding protein (CREB) -2 polyclonal antibody (Santa Cruz Biotechnology, Santa Cruz, CA, USA), mouse anti- GADD153 monoclonal antibody (Santa Cruz Biotechnology), rabbit anti-actin polyclonal antibody (Santa Cruz Biotechnology), Alexa fluor 488 F(ab')$_2$ fragment of goat anti-rabbit IgG (H+L) (Molecular Probes, Leiden, The Netherlands), Alexa fluor 546 F(ab')$_2$ fragment of goat anti-mouse IgG (H+L) (Molecular Probes), Zenon Alexa Fluor 488 Mouse IgG$_1$ Labeling Kit (Invitrogen, Tokyo, Japan), Zenon Alexa Fluor 546 Mouse IgG$_{2a}$ Labeling Kit (Invitrogen), SuperSignal West Femto Maximum Sensitivity Substrate Antibodies (Pierce, Rockford, IL, USA), Running Buffer Solution (Wako), Owl's Electroblot Buffer Kit (Owl, Portsmouth, NH, USA), SuperSep 10% (Wako), bicinchoninic acid (BCA) Protein Assay Kit (Pierce), Immobilon-P (Millipore, Tokyo, Japan), Gel Blot Paper (Schleicher & Schuell, Keene, NH, USA), Sample buffer (Wako), *In situ* apoptosis detection kit (Takara Shuzo, Otsu, Japan), TSA Biotin system (PerkinElmer Life Sciences Inc., Boston, MA, USA), Precision Plus Protein Standards Dual Color (Bio-Rad), Block Ace (Dainippon Pharmaceutical), Can Get Signal (TOYOBO, Osaka, Japan), protease inhibitor cocktail (Sigma, St. Louis, MO, USA), phosphatase inhibitor cocktail I, II (Sigma), and ProLong Gold antifade reagent (Molecular Probes).

Surgical procedure for the gerbil forebrain ischemia

Earlier studies found that hippocampal Cornet d'Ammon (CA)1 pyramidal cells are selectively vulnerable to ischemia and undergo apoptosis after transient ischemia (Kirino, 1982; Kirino and Sano, 1984). In the present study, the gerbils were anesthetized with a mixture of 2.5% isoflurane in 70% N_2O and 30% O_2. The common carotid arteries were exposed, and after completion of the surgical procedures, the isoflurane was discontinued, and 1 min later both carotid arteries were occluded (using Sugita No. 51 temporary aneurysm clips; MIZUHO Co. Ltd., Tokyo, Japan) for 10 min. The body temperature of the animals was maintained at 36.5–37.0 °C using a heating pad with a heating lamp during the operation period and until a righting reflex reappeared. Sham-operated animals were treated in the same manner, except for the absence of occlusion.

Immunohistochemistry

At 12 h, and 1, 3, or 7 days after ischemia, gerbils were anesthetized with sodium pentobarbital (Nembutal, 50 mg/kg, i.p.), and the brains were perfusion-fixed with 4% paraformaldehyde in 0.1 M phosphate buffer (pH 7.4). The brains were removed after 20 min perfusion fixation at 4 °C, then immersed in the same fixative solution overnight at 4 °C. The brains were then immersed in 25% sucrose in 0.1 M phosphate buffer for 24 h, then frozen in powdered dry ice. Serial coronal sections 10 μm thick were cut on a cryostat at −20 °C, and stored at −80 °C until needed for immunostaining.

Brain sections were rehydrated in phosphate buffered saline (PBS), then treated with 0.3% hydrogen peroxidase in methanol. They were then washed three times in PBS, followed by a preincubation with 10% normal goat serum. They were then incubated with primary antibodies overnight at 4 °C. The slides were washed and then incubated with biotinylated anti-mouse IgG or anti-rabbit IgG. They were subsequently incubated with avidin–biotin–peroxidase complex for 30 min and then developed using DAB peroxidase substrate.

For immunostaining, the following primary antibodies were used: a mouse anti-KDEL monoclonal antibody (1:400) and a mouse anti-GADD153 monoclonal antibody (1:100).

Fluorescent double staining

To confirm the cell phenotypes containing BiP, we carried out fluorescent double-staining for an ER-stress marker and cell-phenotype markers. Cell phenotypes containing BiP were detected by means of a Zenon mouse IgG labeling kit. The sections were prepared and fixed as described above, then incubated with a primary antibody for KDEL (at a dilution of 1:150) labeled with Zenon Alexa Fluor 546, and with a primary antibody for either NeuN or GFAP (at a dilution of 1:100 and 1:1, respectively) labeled with Zenon Alexa Fluor 488. After fixation of the tissue sections in 4% paraformaldehyde in PBS, they were mounted in ProLong Gold antifade reagent.

Histological analysis and detection of apoptosis

After sections had been stained with Cresyl Violet, neuronal degeneration was quantified as described previously (Hara et al., 1990). The number of neurons per 1 mm linear length of stratum pyramidale of the hippocampal CA1 subfield (neuronal density) was calculated by counting living neurons (using a microscope) and dividing by the total length of the CA1 cell layer in each section. The average of the values obtained for neuronal density on the two sides was regarded as the neuronal cell density for a given gerbil, according to the method of Kirino et al. (1986). The linear length of the CA1 subfield was measured using Image J (http://rsb.info.nih.gov/ij/download/).

Apoptosis was detected by a terminal deoxynucleotidyl transferase-mediated DNA nick-end labeling (TUNEL) method using an *in situ* apoptosis detection kit. TUNEL signals were amplified with Streptavidin Alexa Fluor 488 conjugate (diluted 1:200) using the TSA Biotin System.

Western blot analysis

At designated time-points after the ischemia, gerbils were killed by cervical dislocation following an overdose of pentobarbital (120 mg/kg body weight, i.p.). The brains were quickly removed and cut into coronal slices 2 mm thick. The hippocampal CA1 subregion, CA3 subregion, dentate gyrus (DG), and cortex were carefully separated from the brains, and quickly frozen in dry ice. For protein extraction, the tissue was homogenized with about eight volumes of RIPA buffer (a chemical reagent to solubilize protein) containing 1% protease inhibitor cocktail and phosphatase inhibitor cocktails. The homogenate was centrifuged at 10,000 r.p.m. for 20 min and the supernatant was used for this study. Assays to determine the protein concentration were performed by comparison with a known concentration of bovine serum albumin, using a BCA Protein Assay Kit.

An aliquot of 5 μg of protein was subjected to 10% sodium dodecyl sulfate–polyacrylamide gel electrophoresis. The separated protein was transferred onto a polyvinylidene difluoride membrane (Immobilon-P; Millipore Corporation, Bedford, MA, USA). For immunoblotting, the following primary antibodies were used: a mouse anti-BiP monoclonal antibody (1:250), a rabbit anti-CREB-2 polyclonal antibody (1:200), and a rabbit anti-actin polyclonal antibody (1:2000). The secondary antibodies used were anti-mouse HRP-conjugated (1:2000) and goat anti-rabbit HRP-conjugated (1:2000). The immunoreactive bands were visualized by means of SuperSignal West Femto Maximum Sensitivity Substrate. The band intensity was measured using a Lumino Imaging Analyzer (FAS-1000; TOYOBO) and Gel Pro Analyzer (Media Cybernetics, Atlanta, GA, USA).

Reverse-transcription polymerase chain reaction (RT-PCR)

Total RNA was isolated from the brain tissues using an RNeasy kit (Qiagen K.K., Tokyo, Japan) according to the manufacturer's protocol. RNA concentrations were determined spectrophotometrically at 260 nm. First-strand cDNA was synthesized in a 20 μl reaction volume using a random primer (Takara, Shiga, Japan) and Moloney murine leukemia virus reverse transcriptase (Invitrogen). PCR was performed in a total volume of 30 μl containing 0.8 μM of each primer, 0.2 mM dNTPs, 3 U *Taq*DNA polymerase (Promega), 2.5 mM $MgCl_2$, and 10× PCR buffer. The amplification conditions for semi-quantitative RT-PCR analysis were as follows: an initial denaturation step (95 °C for 5 min), 22 cycles of 95 °C for 1 min, 55 °C for 1 min, and 72 °C for 1 min, and a final extension step (72 °C for 7 min). The numbers of amplification cycles for the detection of ATF-4 and β-actin were 18 and 15, respectively. The primers used for amplification were as follows: ATF4, 5′-GGACAGATTGGATGTTGGAGAAAATG-3′ and 5′-GGAGATGGCCAATTGGGTTCAC-3′; β-actin, 5′-TCCTCCCTG-GAGAAGAGCTAC-3′ and 5′-TCCTGCTTGCTGATCCACAT-3′. The PCR products were resolved by electrophoresis through a 4.8% (w/v) polyacrylamide gel. The density of each band was quantified using the Scion Image Program (Scion Corporation, Frederick, MD, USA).

Statistical analysis

Data are presented as the means±S.E. Statistical comparisons were made using a Student's *t*-test or one-way ANOVA followed by Dunnett's test [using STAT VIEW version 5.0 (SAS Institute, Cary, NC, USA)]. $P<0.05$ was considered to indicate statistical significance.

RESULTS

Histological assessment of gerbil brain and induction of BiP in the brain after transient forebrain ischemia

We performed a histological assessment of the gerbil brain after transient forebrain ischemia as the first step in clarifying whether ER-stress and induction of BiP is involved in the present model. With Cresyl Violet staining, no neuronal degeneration in the hippocampal CA1 region was detected at either 12 h or 1 day after the ischemia. At 3 days, however, CA1 pyramidal neurons had degenerated (Fig. 1A–C), as reported in previous studies (Kirino, 1982; Kirino and

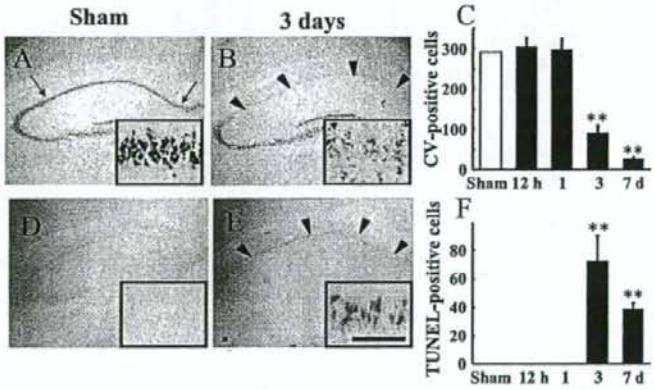

Fig. 1. Representative photomicrographs of hippocampal CA1 subfield, together with analysis of changes in neuronal density of Cresyl Violet–positive cells and TUNEL-positive cells, after transient forebrain ischemia in gerbils. (A, B) Cresyl Violet (CV) staining. (A) Sham operation, striatum pyramidale in the CA1 region (between the arrows). (B) Three days after ischemia. Note marked damage to the CA1 pyramidal cells (arrowheads). (C) Neuronal density (number of cells/mm) of CV-positive cells. (D, E) TUNEL staining. (D) Sham operation. (E) Three days after ischemia. Note marked TUNEL-positive cells among CA1 pyramidal cells (arrowheads). Scale bar=40 μm. (F) Neuronal density (number of cells/mm) of TUNEL-positive cells. Values are expressed as the mean±S.E. (n=3–5). ** $P<0.01$ vs. sham (Dunnett's multiple range test).

Sano, 1984). TUNEL-positive cells were selectively observed in the hippocampal CA1 at 3 days after the ischemia. At 7 days after the ischemia, TUNEL-positive cells had decreased to approximately 50% of the number seen at 3 days (Fig. 1D–F).

BiP, an ER-resident molecular chaperon, is a representative marker of ER-stress, and contains a characteristic COOH-terminal Lys-Asp-Glu-Leu (KDEL) sequence. We therefore performed an immunohistochemical study for BiP using an anti-KDEL monoclonal antibody. Although both BiP and glucose regulated protein (GRP) 94 are detected by this antibody, we obtained evidence that BiP was mainly detected (by means of Western blot analysis in a preliminary test).

Slight immunoreactivity was detected at 12 h after the ischemia in CA1 (versus the sham-operation group). At 1 day, many neurons were quite densely stained, with some neurons showing a very strong immunoreactivity at this

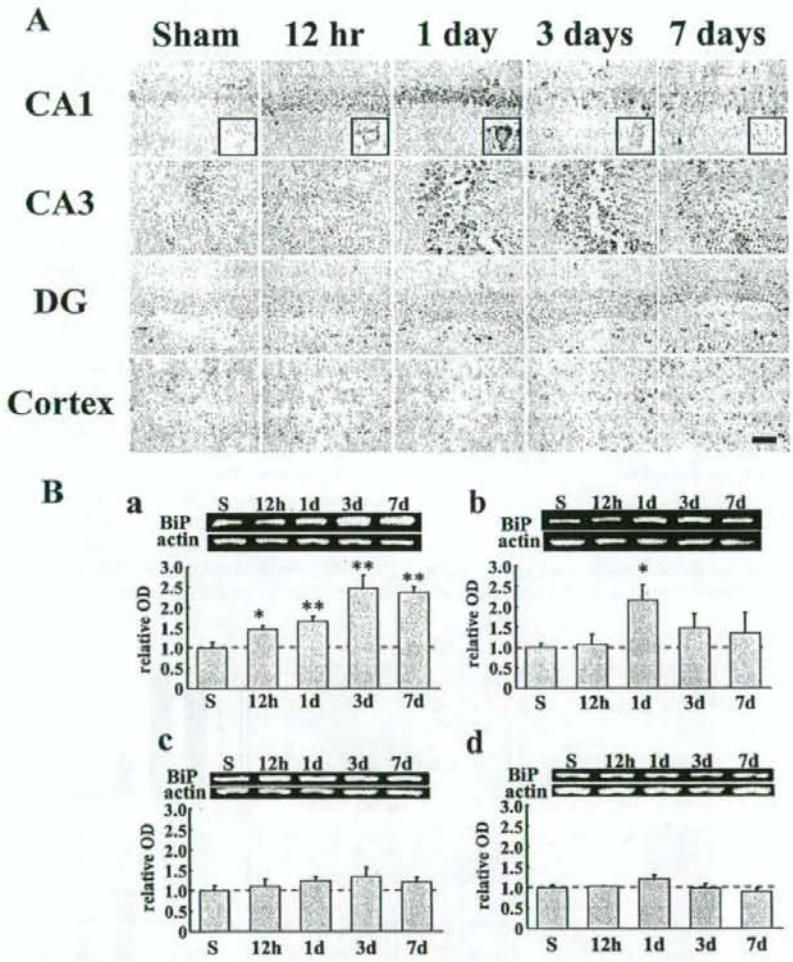

Fig. 2. BiP expression induced by ischemia in hippocampus. Under isoflurane anesthesia, the common carotid arteries were exposed, then occluded bilaterally for 10 min. Brains were analyzed 12 h, and 1, 3, or 7 days after the ischemia. (A) Immunohistochemistry for BiP showed very weak immunoreactivity in the sham-operated brains (Sham). In the hippocampal CA1, immunoreactivity was slightly elevated at 12 h, and peaked at 1 day after ischemia. At 3 and 7 days, almost no immunoreactivity was detected in hippocampal CA1 pyramidal cells. In the hippocampal CA3, immunoreactivity was strong at 1 and 3 days after the ischemia. In the DG and cortex, immunoreactivity was unchanged by ischemia. Squares are higher magnification views of CA1. Scale bar=50 μm (B) By Western blot analysis, BiP was apparently detectable in sham-operated gerbils (Sham). In the hippocampal CA1, BiP was significantly increased at 12 h, then increased progressively to peak at 3 days after the ischemia (a). In the hippocampal CA3, BiP was increased only at 1 day after the ischemia (b). In the DG and cortex, no increases were detected (c, d). Values are expressed as the mean±S.E. * $P<0.05$, ** $P<0.01$ vs. sham ($n=4–9$)

time-point. At 3 days, most of the neurons had degenerated, and the remaining neurons showed positive immunoreactivity. At 1 and 3 days, the immunoreactivity was also increased in CA3. In the DG and cortex, signals for BiP were unchanged (Fig. 2A).

Next, we performed Western blot analysis for BiP using an anti-BiP monoclonal antibody. In this analysis, BiP signals were significantly increased in CA1 at 12 h after the ischemia (the early stage after the ischemia), and the signals increased time-dependently until they reached maximum at 3 days after the ischemia. At 7 days, the signals were hardly changed compared with those at 3 days. BiP signals were increased in CA3 only at the 1-day time-point. In the DG and cortex, BiP signals were unchanged (Fig. 2B). Thus, BiP was induced after ischemia in CA1, but there was a mismatch between the immunohistochemical study and the Western blot analysis regarding the time course of the changes in BiP expression. The peak of BiP expression after ischemia in the CA1 was 1 day and 3 days in immunohistochemistry and Western blots, respectively. Therefore, we investigated the co-localization of BiP with NeuN or GFAP (which are markers of neurons and astrocytes, respectively) at 1 and 7 days after ischemia.

Co-localization of BiP-positive cells

Expression of NeuN was observed in CA1 pyramidal cells at the 1-day time-point, although rarely at 7 days. In contrast, only a slight expression of GFAP was observed at 1 day, but a great number of GFAP-positive cells were observed at 7 days. BiP was co-localized with NeuN at 1 day, although rarely co-localized at 7 days, while BiP was partially co-localized with GFAP at 7 days (Fig. 3).

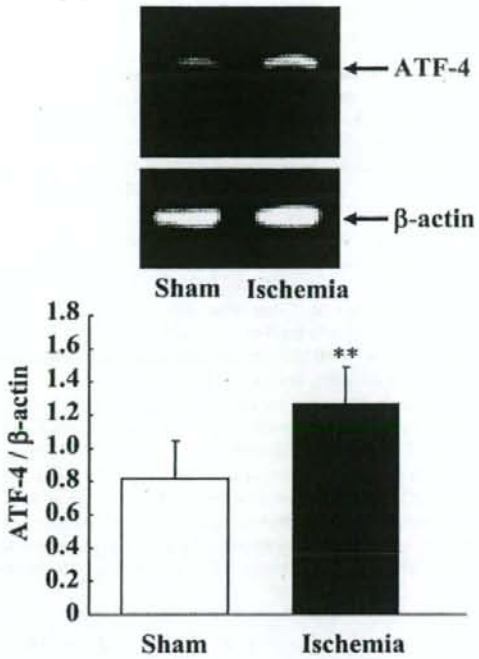

Fig. 4. ATF-4 expression induced by ischemia in hippocampus. The common carotid arteries were occluded bilaterally for 10 min, and the brains were analyzed 6 h after the ischemia. β-Actin mRNA is shown as an internal control. The level of ATF-4 mRNA was increased at 6 h after the ischemia.

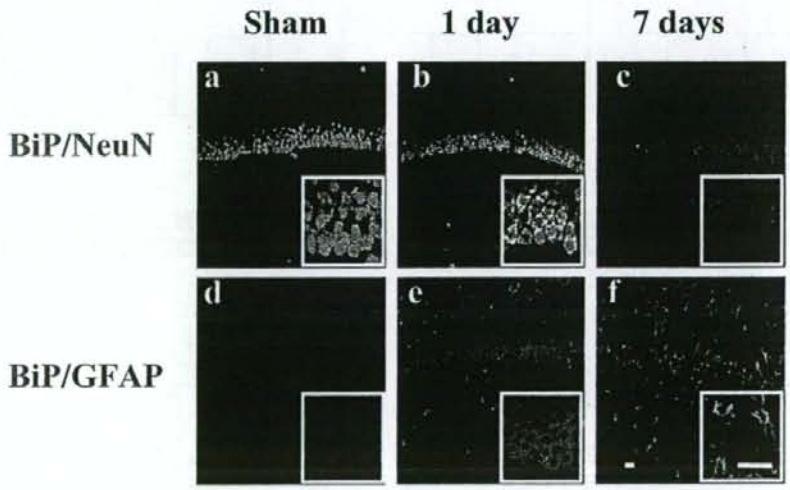

Fig. 3. Co-localization of BiP with NeuN or GFAP. Brains were taken for analysis at 1 or 7 days after ischemia. In the hippocampal CA1, BiP-positive cells were similar in population and morphology to NeuN-positive cells, but not to GFAP-positive cells (both in the sham-operated brains and at 1 day after ischemia) (a, b, d, e). At 7 days, no NeuN immunoreactivity was detected, and signals for BiP and NeuN were not co-localized (c), whereas signals for BiP and GFAP were detected and co-localized in the stratum oriens, stratum radiatum, and stratum lacunosum-moleculare (f). Scale bar=25 μm.

Expressions of other ER-stress markers after ischemia

Next, to try to confirm the involvement of ER-stress in this model, we assessed other ER-stress markers. In this study, we examined one of these apoptosis signals (the CHOP/GADD153-mediated pathway) by evaluating CHOP and ATF-4, which is upstream of CHOP, using immunohistochemistry, RT-PCR analysis, and Western blot analysis.

RT-PCR analysis showed that ATF-4 mRNA was significantly induced at 6 h after the ischemia in CA1 (Fig. 4). In our Western blot analysis, ATF-4 signals were significantly increased at 1 day after the ischemia in CA1. In CA3, ATF-4 signals tended to be increased at 1 day after the ischemia (P=0.06). In the DG and cortex, however, ATF-4 signals were unchanged (Fig. 5).

In our immunohistochemical study, the expression of CHOP, a proapototic marker, was condensed to within the nuclei of CA1 pyramidal cells. The number of CHOP-positive cells reached maximum at 3 days after the ischemia in CA1. In CA3, CHOP immunoreactivity was increased at 12 h and 1 day after the ischemia. In the DG and cortex, CHOP immunoreactivity was unchanged (Fig. 6). Overexpression of CHOP and microinjection of CHOP protein have been reported to lead to cell-cycle arrest and/or apoptosis (Barone et al., 1994; Matsumoto et al., 1996; Maytin et al., 2001; Oyadomari et al., 2001; Gotoh et al., 2002). In the present study, CHOP induction in CA1 occurred at the same time as cell death.

Co-localization of CHOP and TUNEL

Interestingly, despite CHOP expression being detected at 12 h and 1 day in CA3, no cell death was observed at these time-points. We therefore investigated the co-localization of TUNEL (a marker of apoptosis) and CHOP in CA1 and CA3. CHOP was co-localized with TUNEL at 3 days after the ischemia in CA1, but not at 12 h in CA3 (Fig. 7). Increased CHOP is thought to contribute to the pathogenesis of ischemic sequelae, but it remains to be elucidated whether and how CHOP-induction and ER-stress-mediated apoptosis are related in the development of such events.

DISCUSSION

In the present study, we set out to clarify the involvement of ER-stress in hippocampal CA1-selective neuronal cell death using a gerbil model of transient forebrain ischemia. BiP expression in hippocampal CA1 induced early stage

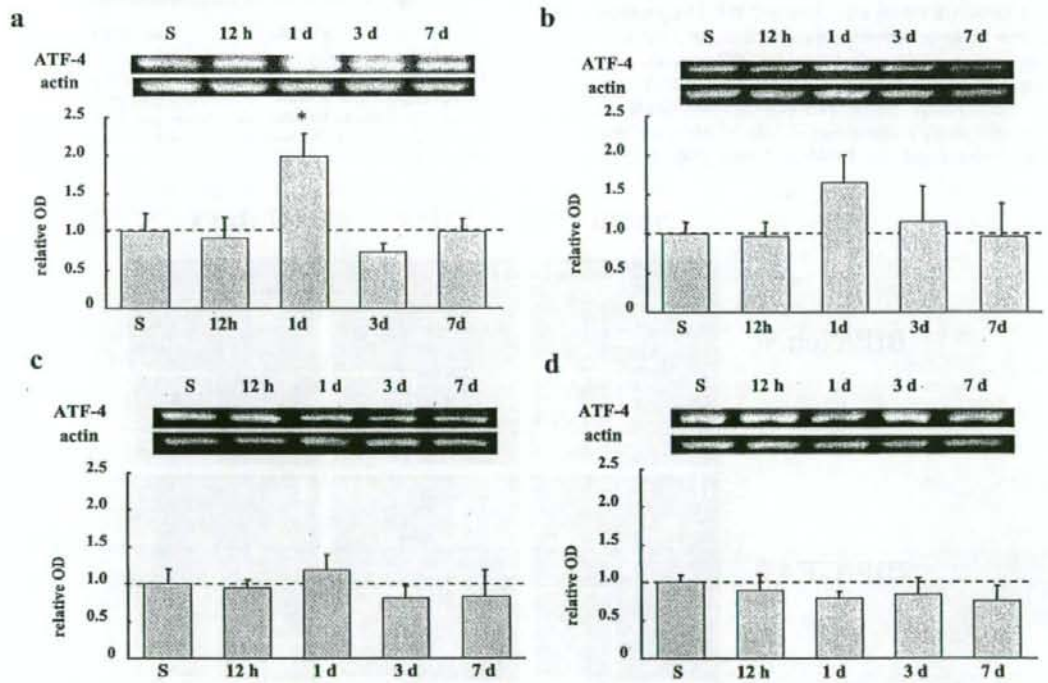

Fig. 5. ATF-4 expression induced by ischemia in the hippocampus. By Western blot analysis, ATF-4 was apparently detectable in sham-operated gerbils (Sham). In the hippocampal CA1, ATF-4 was increased only at 1 day after the ischemia (a). In the hippocampal CA3, ATF-4 was slightly increased at 1 day after the ischemia (b). In the DG and cortex, no increases were detected (c, d). Values are expressed as the mean±S.E. * P<0.05, ** P<0.01 vs. sham (S) (n=4–9).

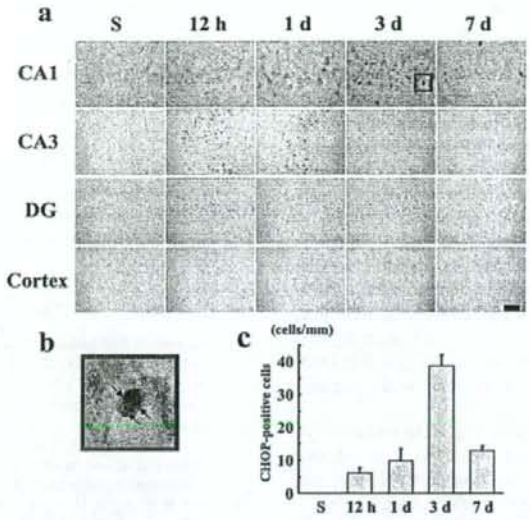

Fig. 6. CHOP expression induced by ischemia. Occlusion of common carotid arteries (bilaterally) and analysis of brains were as described in Fig. 2. Immunohistochemistry for CHOP showed no immunoreactivity in the sham-operated gerbils (S) (a). In the hippocampal CA1, immunoreactivity was slightly increased at 1 day, and peaked at 3 days after the ischemia. At 7 days, almost no immunoreactivity was detected in hippocampal CA1 pyramidal cells. In the hippocampal CA3, immunoreactivity was strong at both 12 h and 1 day after the ischemia. At 3 and 7 days, no immunoreactivity was detected in the hippocampal CA3 pyramidal cells. In the DG and cortex, no immunoreactivity was detected. Square: area shown at higher magnification in (b). Scale bar=50 μm. (b) Representative photomicrograph of CHOP-positive cells in the hippocampal CA1. The signal has been condensed to the nucleus (arrows). (c) Quantitative analysis of CHOP-positive cells in hippocampal CA1. CHOP-positive cells increased progressively from 12 h to peak at 3 days after the ischemia. Values are expressed as the mean±S.E. (n=3–5).

(12 h and 1 day, which did not show any morphological damage) after transient forebrain ischemia. Our results demonstrated that a significant burden of ER-stress at the early stage after the ischemia was involved in the execution of the cell death. Reportedly, accumulation of unfolded protein in the ER lumen, phosphorylation of eIF2α, inhibition of protein synthesis, and calcium depletion from the ER lumen all suggest an active role for the ER in neuronal cell death after ischemia (Althausen et al., 2001; DeGracia et al., 2002; Hu et al., 2000; Nowak et al., 1985; Paschen and Frandsen, 2001). However, this is the first report of an involvement of ER-stress in transient global ischemia-induced cell death in the gerbil CA1 subfield.

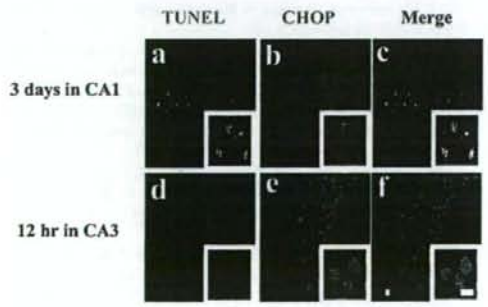

Fig. 7. Co-localization of CHOP-and TUNEL-positivity in hippocampus. In the hippocampal CA1, both population and morphology were similar between CHOP-positive cells and TUNEL-positive cells at 3 days after the ischemia (a, b, c). In the hippocampal CA3, signals for CHOP and TUNEL were not co-localized at 12 h after the ischemia (d, e, f). Scale bar=10 μm.

The expression of BiP, an ER-resident molecular chaperon and a representative marker of ER-stress, was at a low level in CA1, CA3, DG, and cortex in gerbils not exposed to ischemia, but it was upregulated at an early stage after ischemia in both CA1 and CA3 (Fig. 2). Other proteins were also upregulated in dying neurons. One of these proteins is B/K protein, which is a newly identified member of double C2-like domain protein family. The hippocampal region showing the early and significant increase of B/K protein expression in kainite-induced seizure model was the CA3 that has been known to be vulnerable to kainite-induced excitotoxicity (Jang et al., 2004). Furthermore, the spatiotemporal pattern of B/K protein expression in a kainite seizure model was similar to that of BiP, and confocal microscopic examination demonstrated the coexpression of two proteins (Jang et al., 2004). In the Western blot analysis, BiP expression was at its maximum at 3 and 7 days (with almost all pyramidal cells dead) in CA1. The immunohistochemistry and Western blot analysis was consistent in that in each, upregulation of BiP was detected in CA1 at the early stage after the ischemia, when neuronal cell death had not occurred. However, the expressions at the later stage (when neuronal cell death had occurred) showed a mismatch between these two meth-

ods. It is widely known that glial cells show tolerance against ischemia. Therefore, we thought glial cells might be more involved in the later phase, and so we investigated the co-localization of BiP with NeuN or GFAP. In this examination, BiP expression was not detected in neuronal cells after neuronal cell death, but was partially detected in astrocytes (Fig. 3). As described above, astrocytes are more tolerant to ER-stress-mediated cell death than other cells, such as neurons. A possible mechanism might involve old astrocyte specifically induced substance (OASIS), a transmembrane bZIP transcriptional factor with a structure similar to that of ATF-6. OASIS is coded by a particular gene expressed specifically in astrocytes (Kondo et al., 2005). These findings suggest that an ER-stress response may be present in astrocytes, which show tolerance against ischemia, in the later phase after ischemia, possibly leading to the activation of a defense mechanism against ER-stress.

Normally, CHOP is ubiquitously expressed at very low levels (Ron and Habener, 1992). However, it is robustly expressed in a wide variety of cells by perturbations that induce stress (Ron and Habener, 1992), and CHOP$^{-/-}$ cells are resistant to ER-stress-mediated apoptosis (Zinszner et al., 1988; Oyadomari et al., 2001; Gotoh et al., 2002). In our study, we focused on one of the ER-derived apoptosis signals, the CHOP/GADD153-mediated pathway. The expression of ATF-4 was significantly increased at 1 day after ischemia in CA1, and tended to be increased at 1 day in CA3 (Fig. 5). In our immunohistochemical study, CHOP expression was significantly increased at 1 day after the ischemia in CA1, reaching maximum at 3 days after the ischemia. In CA3, its expression was significantly increased at both 12 h and 1 day (Fig. 6). The time course of these changes in ATF-4 and CHOP in CA1 is consistent with that of the morphological changes induced by ischemia. Possibly, the burden of significant ER-stress at an early stage during or after ischemia may lead to a failure of the defense mechanism, and a subsequent activation of apoptosis signals at 1 day or so after the ischemia. However, there are no direct evidences regarding a role of CHOP in CA3 after ischemia. Therefore, further experiments will be needed to clarify the detailed mechanism.

Interestingly, CHOP expression was detected at 12 h after the ischemia in CA3, when cell death had not yet occurred. When we investigated the co-localization of TUNEL, a representative marker of apoptosis, with CHOP, we found co-localization at 3 days after the ischemia in CA1, but not at 12 h in CA3 (Fig. 7). Although CHOP may play a role in the induction of ER-derived apoptosis (Fawcett et al., 1996; Cortes-Canteli et al., 2001), induction of CHOP alone is not sufficient for the activation of such apoptosis, and so an unknown signal downstream of CHOP may trigger detrimental downstream events. The involvement of CHOP in ER-derived apoptosis signaling has been reported by several researchers (Harding et al., 2000; Oyadomari and Mori, 2004; Hayashi et al., 2005; Silva et al., 2005). Furthermore, ER-stress sensor double-stranded PERK, ATF6, and inositol-requiring enzyme 1 (IRE1), which exist on the ER membrane, participate in the induction of CHOP. Taken together, the above evidence suggests that the expression of CHOP in the hippocampal CA1 subfield of the gerbil after transient ischemia is mainly regulated at the transcriptional level, and that CHOP may play an important role in ER-derived apoptosis signaling.

CONCLUSION

In conclusion, we suggest that ER-stress is involved in the CA1-selective neuronal cell death we observed in a gerbil transient forebrain ischemia model.

REFERENCES

Althausen S, Mengesdorf T, Mies G, Olah L, Nairn AC, Proud CG, Paschen W (2001) Changes in the phosphorylation of initiation factor eIF-2alpha, elongation factor eEF-2 and p70 S6 kinase after transient focal cerebral ischaemia in mice. J Neurochem 78: 779–787.

Barone MV, Crozat A, Tabaee A, Philipson L, Ron D (1994) CHOP (GADD153) and its oncogenic variant, TLS-CHOP, have opposing effects on the induction of G1/S arrest. Genes Dev 15:453–464.

Calfon M, Zeng H, Urano F, Till JH, Hubbard SR, Harding HP, Clark SG, Ron D (2002) IRE1 couples endoplasmic reticulum load to secretory capacity by processing the XBP-1 mRNA. Nature 415: 92–96.

Cortes-Canteli M, Pignatelli M, Santos A, Perez-Castillo A (2001) CCAAT/enhancer-binding protein beta plays a regulatory role in differentiation and apoptosis of neuroblastoma cells. J Biol Chem 277:5460–5467.

DeGracia DJ, Kumar R, Owen CR, Krause GS, White BC (2002) Molecular pathways of protein synthesis inhibition during brain reperfusion: implications for neuronal survival or death. J Cereb Blood Flow Metab 22:127–141.

Fawcett TW, Eastman HB, Martindale JL, Holbrook NJ (1996) Physical and functional association between GADD153 and CCAAT/enhancer-binding protein beta during cellular stress. J Biol Chem 271:14285–14289.

Gotoh T, Oyadomari S, Mori K, Mori M (2002) Nitric oxide-induced apoptosis in RAW 264.7 macrophages is mediated by endoplasmic reticulum stress pathway involving ATF6 and CHOP. J Biol Chem 277:12343–12350.

Hara H, Onodera H, Yoshidomi M, Matsuda Y, Kogure K (1990) Staurosporine, a novel protein kinase C inhibitor, prevents post-ischemic neuronal damage in the gerbil and rat. J Cereb Blood Flow Metab 10:646–653.

Harding HP, Novoa I, Zhang Y, Zeng H, Wek R, Schapira M, Ron D (2000) Regulated translation initiation controls stress-induced gene expression in mammalian cells. Mol Cell 6:1099–1108.

Harding HP, Calfon M, Urano F, Novoa I, Ron D (2002) Transcriptional and translational control in the mammalian unfolded protein response. Annu Rev Cell Dev Biol 18:575–599.

Hayashi T, Saito A, Okuno S, Ferrand-Drake M, Dodd RL, Chan PH (2005) Damage to the endoplasmic reticulum and activation of apoptotic machinery by oxidative stress in ischemic neurons. J Cereb Blood Flow Metab 25:41–53.

Hu BR, Martone ME, Jones YZ, Liu CL (2000) Protein aggregation after transient cerebral ischemia. J Neurosci 20:3191–3199.

Ito D, Tanaka K, Suzuki S, Dembo T, Kosakai A, Fukuuchi Y (2001) Up-regulation of the Ire1-mediated signaling molecule, BiP, in ischemic rat brain. Neuroreport 12:4023–4028.

Jang YS, Lee MY, Choi SH, Kim MY, Chin H, Jeong SW, Kim IK, Kwon OJ (2004) Expression of B/K protein in the hippocampus of kainate-induced rat seizure model. Brain Res 999:203–211.

Kirino T (1982) Delayed neuronal death in the gerbil hippocampus following ischemia. Brain Res 239:57–69.

Kirino T, Sano K (1984) Fine structural nature of delayed neuronal death following ischemia in the gerbil hippocampus. Acta Neuropathol (Berl) 62:209–218.

Kirino T, Tamura A, Sano K (1986) A reversible type of neuronal injury following ischemia in the gerbil hippocampus. Stroke 17:455–459.

Kondo S, Murakami T, Tatsumi K, Ogata M, Kanemoto S, Otori K, Iseki K, Wanaka A, Imaizumi K (2005) OASIS, a CREB/ATF-family member, modulates UPR signalling in astrocytes. Nat Cell Biol 7:186–194.

Kumar R, Azam S, Sullivan JM, Owen C, Cavener DR, Zhang P, Ron D, Harding HP, Chen JJ, Han A, White BC, Krause GS, DeGracia DJ (2001) Brain ischemia and reperfusion activates the eukaryotic initiation factor 2alpha kinase, PERK. J Neurochem 77:1418–1421.

Leroux L, Desbois P, Lamote L, Duvillie B, Cordonnier N, Jackerott M, Jami J, Bucchini D, Joshi RL (2001) Compensatory responses in mice carrying a null mutation for Ins1or Ins2. Diabetes 50:S150–S153.

Ma Y, Hendershot LM (2001) The unfolding tale of the unfolded protein response. Cell 107:827–830.

Matsumoto M, Minami M, Takeda K, Sakao Y, Akira S (1996) Ectopic expression of CHOP (GADD153) induces apoptosis in M1 myeloblastic leukemia cells. FEBS Lett 21:143–147.

Maytin EV, Ubeda M, Lin JC, Habener JF (2001) Stress-inducible transcription factor CHOP/gadd153 induces apoptosis in mammalian cells via p38 kinase-dependent and -independent mechanisms. Exp Cell Res 15:193–204.

Morimoto N, Oida Y, Shimazawa M, Miura M, Kudo T, Imaizumi K, Hara H (2007) Involvement of endoplasmic reticulum stress after middle cerebral artery occlusion in mice. Neuroscience 147:957–967.

Mouw G, Zechel JL, Gamboa J, Lust WD, Selman WR, Ratcheson RA (2003) Activation of caspase-12, an endoplasmic reticulum resident caspase, after permanent focal ischemia in rat. Neuroreport 14:183–186.

Nakagawa T, Zhu H, Morishima N, Li E, Xu J, Yankner BA, Yuan J (2000) Caspase-12 mediates endoplasmic-reticulum-specific apoptosis and cytotoxicity by amyloid-beta. Nature 403:98–103.

Nowak TS Jr, Fried RL, Lust WD, Passonneau JV (1985) Changes in brain energy metabolism and protein synthesis following transient bilateral ischemia in the gerbil. J Neurochem 44:487–494.

Oyadomari S, Takeda K, Takiguchi M, Gotoh T, Matsumoto M, Wada I, Akira S, Araki E, Mori M (2001) Nitric oxide-induced apoptosis in pancreatic beta cells is mediated by the endoplasmic reticulum stress pathway. Proc Natl Acad Sci U S A 98:10845–10850.

Oyadomari S, Mori M (2004) Roles of CHOP/GADD153 in endoplasmic reticulum stress. Cell Death Differ 11:381–389.

Paschen W, Frandsen A (2001) Endoplasmic reticulum dysfunction: a common denominator for cell injury in acute and degenerative diseases of the brain? J Neurochem 79:719–725.

Paschen W, Aufenberg C, Hotop S, Mengesdorf T (2003) Transient cerebral ischemia activates processing of xbp1 messenger RNA indicative of endoplasmic reticulum stress. J Cereb Blood Flow Metab 23:449–461.

Ron D, Habener JF (1992) CHOP, a novel developmentally regulated nuclear protein that dimerizes with transcription factors C/EBP and LAP and functions as a dominant-negative inhibitor of gene transcription. Genes Dev 6:439–453.

Silva RM, Ries V, Oo TF, Yarygina O, Jackson-Lewis V, Ryu EJ, Lu PD, Marciniak SM, Ron D, Przedborski S, Kholodilov N, Greene LA, Burke RE (2005) CHOP/GADD153 is a mediator of apoptotic death in substantia nigra dopamine neurons in an in vivo neurotoxin model of parkinsonism. J Neurochem 95:974–986.

Takeda K, Matsuzawa A, Nishitoh H, Ichijo H (2003) Roles of MAPKKK ASK1 in stress-induced cell death. Cell Struct Funct 28:23–29.

Tamatani M, Matsuyama T, Yamaguchi A, Mitsuda N, Tsukamoto Y, Taniguchi M, Che YH, Ozawa K, Hori O, Nishimura H, Yamashita A, Okabe M, Yanagi H, Stern DM, Ogawa S, Tohyama M (2001) ORP150 protects against hypoxia/ischemia-induced neuronal death. Nat Med 7:317–323.

Zinszner H, Kuroda M, Wang X, Batchvarova N, Lightfoot RT, Remotti H, Stevens JL, Ron D (1988) CHOP is implicated in programmed cell death in response to impaired function of the endoplasmic reticulum. Genes Dev 12:982–995.

(Accepted 16 October 2007)
(Available online 13 November 2007)

BRAIN RESEARCH 1208 (2008) 217–224

available at www.sciencedirect.com

ScienceDirect

www.elsevier.com/locate/brainres

BRAIN RESEARCH

Research Report

Induction of BiP, an ER-resident protein, prevents the neuronal death induced by transient forebrain ischemia in gerbil

Y. Oida[a], H. Izuta[a], A. Oyagi[a], M. Shimazawa[a], T. Kudo[b], K. Imaizumi[c], H. Hara[a,*]

[a]Department of Biofunctional Evaluation, Molecular Pharmacology, Gifu Pharmaceutical University, 5-6-1 Mitahora-higashi, Gifu 502-8585, Japan

[b]Department of Clinical Neuroscience, Psychiatry, Graduate School of Medicine, Osaka University, 2-2 Yamadaoka, Suita, Osaka 565-0871, Japan

[c]Division of Molecular and Cellular Biology, Department of Anatomy, Faculty of Medicine, University of Miyazaki, Kiyotake, Miyazaki 889-1692, Japan

ARTICLE INFO

Article history:
Accepted 17 February 2008
Available online 4 March 2008

Keywords:
Apoptosis
ER-stress
Immunoglobulin heavy chain binding protein (BiP)
Ischemia
Neuronal cell death

ABSTRACT

Endoplasmic reticulum (ER) stress, which is caused by the accumulation of unfolded proteins in the ER lumen, is associated with stroke and neurodegenerative diseases such as Parkinson's and Alzheimer's diseases. We evaluated the effect of a selective inducer of immunoglobulin heavy chain binding protein (BiP) (BiP inducer X; BIX) against both tunicamycin-induced cell death (in SH-SY5Y cells) and the effects of global transient forebrain ischemia (in gerbils). BIX significantly induced BiP expression both *in vitro* and *in vivo*. Pretreatment with BIX at 2 or 5 μM reduced the cell death induced by tunicamycin in SH-SY5Y cells. In gerbils subjected to forebrain ischemia, prior treatment with BIX (intracerebroventricular injection at 10 or 40 μg) protected against cell death and decreased TUNEL-positive cells in the hippocampal CA1 subfield. These findings indicate that this selective inducer of BiP could be used to prevent the neuronal damage both *in vitro* and *in vivo*.

1. Introduction

In eukaryotes, the endoplasmic reticulum (ER) provides a contained environment for the synthesis and modification of both membrane proteins and proteins destined to be secreted. These post-translational modifications, including disulfide-bond formation and N-linked glycosylation, play important roles in the subsequent folding and oligomeric assembly of proteins (Helenius, 1994). Disruption of the processing of ER proteins leads to activation of the ER-stress pathway and to excess ER stress, resulting in programmed cell death. ER stress have been implicated in the progression of a number of human diseases, including Alzheimer's, Huntington's, and Parkinson's diseases, and type-1 diabetes (Katayama et al., 2001; Nishitoh et al., 2002; Ryu et al., 2002; Oyadomari et al., 2002).

Immunoglobulin heavy chain binding protein (BiP) is one of the molecular chaperones localized to the ER membrane, and is a highly conserved member of the 70-kDa heat shock protein family (Lee, 1992, 2001). BiP serves to restore folding of misfolded or incompletely assembled proteins (Helenius,

* *Corresponding author.* Fax: +81 58 237 8596.
E-mail address: hidehara@gifu-pu.ac.jp (H. Hara).

Abbreviations: ASNS, asparagine synthetase; ATF6, activating transcription factor 6; BiP, immunoglobulin heavy chain binding protein; CHOP, C/EBP homologous protein; ECACC, European Collection of Cell Cultures; EDEM, ER degradation-enhancing α-mannosidase-like protein; ERdj4/MDG1, ER-localized DnaJ4/microvascular differentiation gene 1; GRP94, glucose-regulated protein 94; $p58^{IPK}$, protein kinase inhibitor of 58 kDa; UPR, unfolded protein response; XBP-1, X-box binding protein 1

0006-8993/$ – see front matter © 2008 Elsevier B.V. All rights reserved.
doi:10.1016/j.brainres.2008.02.068

1994; Kuznetsov et al., 1997; Klausner and Sitia, 1990). Previous reports showed that induction of BiP prevents the neuronal death induced by ER stress (Katayama et al., 1999; Yu et al., 1999; Rao et al., 2002; Reddy et al., 2003).

It is well known that in the gerbil, a brief period of global brain ischemia causes selective cell death in hippocampal CA1 pyramidal neurons some 3 to 4 days after reperfusion (Kirino 1982; Kirino and Sano, 1984; Kirino et al., 1986). Other neurons, such as parietal cortical or hippocampal CA3 neurons, are much less vulnerable. On the other hand, occlusion of the middle cerebral arteries (MCA) in mice and rats results in widespread stroke in the ipsilateral cortex and striatum due to ischemia. Recently, protein aggregation in the ER after focal brain ischemia and reperfusion was observed using electron microscopy analysis (Leroux et al., 2001). Further, it has been found that BiP expression is up-regulated by ischemia in both focal and global transient ischemia models (Ito et al., 2001; Shibata et al., 2003; Tajiri et al., 2004). Similarly, in our previous report ER stress was induced after global ischemia in gerbils (Oida et al., 2008). Interestingly, in the ischemic focus of the infarcted brain of a patient who died after the onset of stroke, expression of oxygen regulated proteins (ORP) 150 (an ER-associated chaperone) was detected in neurons and astrocytes, indicating that ER stress may be involved in ischemic disturbance (Tamatani et al., 2001).

BIX (BiP inducer X) is a chemical compound, 1-(3,4-dihydroxy-phenyl)-2-thiocyanato-ethanone (Fig. 1), and was chosen as an inducer of BiP mRNA using a BiP reporter assay system (Kudo et al., 2008). Our previous report showed that BIX (a) selectively induces BiP in SK-N-SH cells and (b) reduces the area of infarction and the neuronal cell death due to focal cerebral ischemia in mice (Kudo et al., 2008). However, it is unknown whether BIX protects against cell death in the hippocampus (such as the CA1 subfield) after global forebrain ischemia.

Therefore, in the present study we examined the effects of BIX against two types of neuronal cell death: that induced by tunicamycin, an ER-stress inducer, in SH-SY5Y cells and that induced in the hippocampal CA1 subfield after transient global forebrain ischemia in gerbils.

2. Results

2.1. *Effects of BIX on BiP expression and against the cell death induced by ER stress in SH-SY5Y cells*

We first examined whether BIX induces BiP protein in SH-SY5Y cells. BIX at 5 μM significantly up-regulated BiP expression (versus the vehicle-treated group), whereas at 1 μM it did not alter BiP expression (Fig. 2). Next, to determine whether BIX has the ability to protect against ER stress, we examined the effect

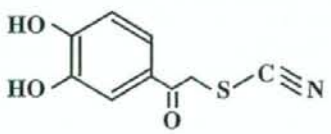

Fig. 1 – Chemical structure of BiP inducer X (BIX), 1-(3,4-dihydroxy-phenyl)-2-thiocyanato-ethanone.

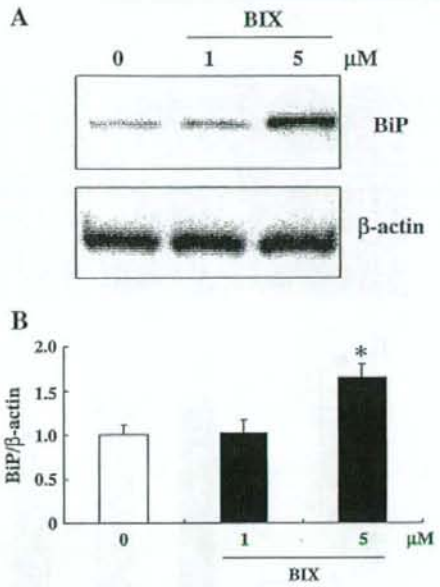

Fig. 2 – Effects of BIX on BiP expression (as assessed using western blot) in SH-SY5Y cells. (A) Induction of BiP expression in SH-SY5Y cells after 24-h treatment with 1, 2 or 5 μM BIX is shown by western blot against anti-BiP/GRP78 antibody and anti-β-actin antibody. (B) BiP expression was quantified by densitometry and corrected by reference to β-actin. The level of BiP protein increased after treatment with BIX at 5 μM. Data represent means and standard error ($n=4$). *$p<0.05$ vs. Control (Student's t-test).

of BIX on the cell death induced by a protein glycosylation inhibitor, tunicamycin, at 2.0 μg/ml. Fluorescence micrographs of Hoechst 33342 and YO-PRO-1 staining are shown in Fig. 3A. BIX (at both 2 and 5 μM) protected against the cell death induced by tunicamycin (Fig. 3B). On the other hand, treatments with BIX (1 to 5 μM) alone did not affect cell viability in SH-SY5Y cells (Fig. 3B).

2.2. *Effect of BIX on BiP mRNA in vivo*

We next investigated whether BIX induces BiP mRNA in gerbils. We detected BiP mRNA by RT-PCR in both normal gerbil brain and human neuroblastoma SK-N-SH cells following treatment with ER-stress inducer (Ca^{2+}-ATPase inhibitor) thapsigargin (Fig. 4A). Furthermore, BiP mRNA was significantly induced in the hippocampus by intracerebroventricular injection of BIX (40 μg/5 μl) at 6 h after its injection (versus the vehicle-treated group) (Fig. 4B).

2.3. *Effect of BIX on the neuronal cell death in the hippocampal CA1 subfield induced by ischemia*

We investigated whether BIX protects against the neuronal cell death induced in gerbils by ischemia and reperfusion (Fig. 5). To judge from our cresyl violet staining, intracerebroventricular

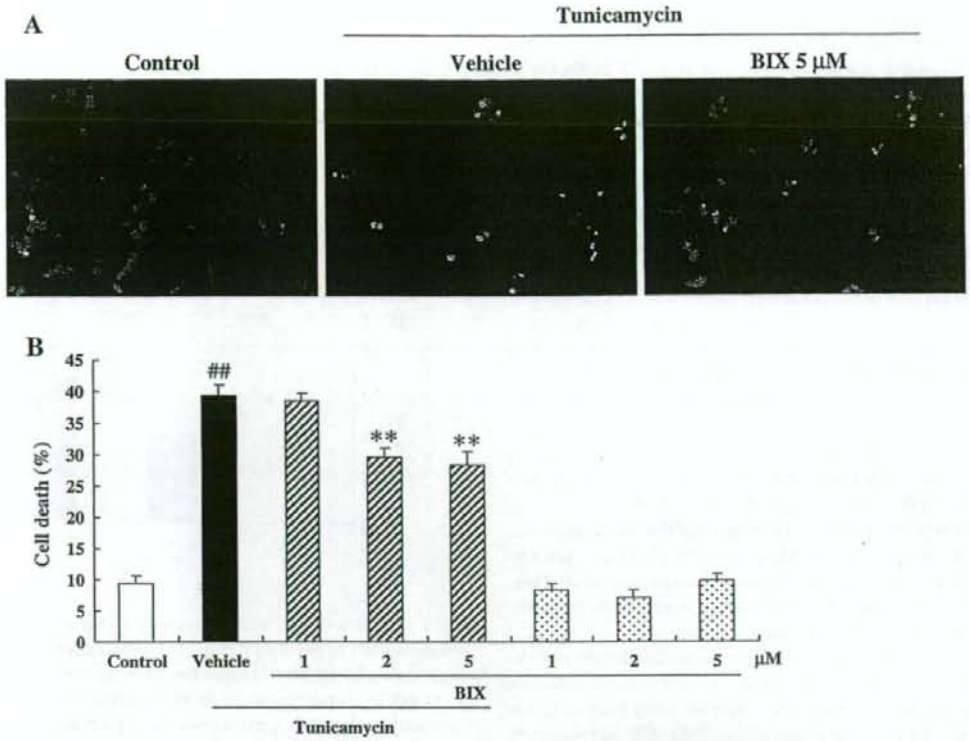

Fig. 3 – Neuroprotective effect of BIX against ER stress-induced cell death in SH-SY5Y cells. SH-SY5Y cells were pre-treated with vehicle or with BIX at 1 to 5 μM for 24 h, followed by 24 h additional incubation with 2.0 μg/ml tunicamycin. (A) Fluorescence micrographs of Hoechst and YO-PRO-1 staining at 24 h after tunicamycin stimulation showed that pretreatment with 5 μM BIX reduced apoptotic cell death (vs. vehicle). (B) The number of dead cells was increased at 24 h after tunicamycin treatment. Pretreatment of cells with BIX at 2 or 5 μM significantly reduced the cell death (vs. vehicle). Data represent means and standard error ($n=6$). ##$p<0.01$ vs. Control, **$p<0.01$ vs. Vehicle (Dunnett's test).

pretreatment with BIX at 10 μg/animal tended (non-significantly; $P=0.11$) to protect against neuronal cell death in the hippocampal CA1 subfield at 7 days after the ischemia (versus the vehicle-treated group), whereas a higher dose (40 μg) offered significant protection (Fig. 5B). On the basis of NeuN-staining, BIX (10 and 40 μg) protected cells against neuronal cell death (Fig. 5C).

2.4. *TUNEL assay*

To determine whether ischemia-induced neuronal cell death in the hippocampal CA1 subfield can be prevented by BIX in gerbils, we detected TUNEL-positive cells after ischemia (much as we had done using cresyl violet- and NeuN-staining methods). Microscope photographs showing TUNEL-staining of cells in the hippocampal CA1 subfield are presented in Fig. 6A. The sham group showed no TUNEL-staining. On the other hand, the control ischemia group showed a large number of TUNEL-positive cells in the hippocampal CA1 subfield at 7 days after ischemia, while prior intracerebroventricular injection of BIX significantly reduced this effect at both 10 and 40 μg (Fig. 6B).

3. Discussion

In the present study, we evaluated the protective effects of BIX (a selective inducer of BiP) (Kudo et al., 2008) against *in vitro* and *in vivo* neuronal cell death (in SH-SY5Y cells and in the hippocampal CA1 subfield in a gerbil transient forebrain ischemia model, respectively).

In SH-SY5Y cells, BIX at 5 μM up-regulated BiP expression, while at 2 and 5 μM it protected against the cell death induced by tunicamycin. Tunicamycin is an ER-stress inducer, and it blocks the synthesis of all N-linked glycoproteins (*N*-glycans) and causes cell-cycle arrest in the G1 phase (Brewer et al., 1999). There was good consistency between the concentration that caused BiP induction and those that were protective against neuronal cell death. In our previous report (Kudo et al., 2008); (a) BIX was found to be a selective inducer of BiP, and at 1 to 50 μM it induced BiP mRNA and protein, with the maximum induction of BiP occurring at 4 h after BIX treatment; (b) although BIX (5 μM) also induced GRP94, calreticulin, and CHOP, their inductions were less marked than that of BiP; (c) on the other hand, ERdj4/MDG1, EDEM, p58^{IPK}, and ASNS mRNA were

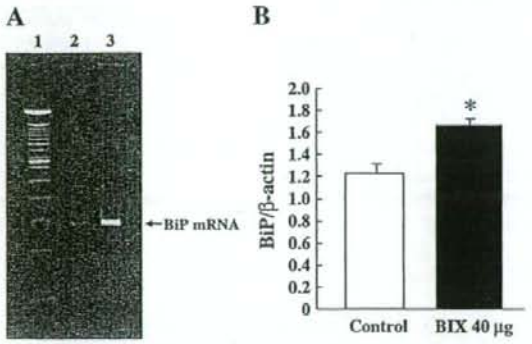

Fig. 4 – Effects of BIX against BiP mRNA induction (as assessed using RT-PCR) *in vivo*. Gerbils were euthanized by cervical dislocation under anesthesia, then brains were quickly removed and the hippocampus carefully separated. SK-N-SH cells were treated with an ER-stress inducer, thapsigargin. (A) Detection of BiP mRNA in normal brain and SK-N-SH cells using RT-PCR. Individual lanes indicate 100 bp ladder marker (Lane 1), normal brain (Lane 2), and SK-N-SH cells with thapsigargin stimulation (Lane 3). (B) Intracerebroventricular injection of BIX (40 μg/5 μl) significantly induced BiP mRNA in the hippocampus at 6 h after the injection (vs. vehicle-treated group). Values are expressed as the mean and standard error (n=5–8). *p<0.05 vs. Control.

scarcely induced at all by BIX; (d) even a high dosage of BIX (50 μM) did not induce genes mediated by non-ATF6 pathways; (e) BIX at 5 μM protected against the cell death induced by tunicamycin in SK-N-SH cells. In the present study, BIX was confirmed to increase BiP expression and protect against neuronal cell death *in vitro* (this time using SH-SY5Y cells).

BiP is one of the molecular chaperones and is induced by ER stress. Expression of BiP protects against the neuronal cell death induced by ER stress (Rao et al., 2002), while degradation of BiP mRNA promotes neuronal death in response to calcium release from the ER (Gomer et al., 1991). Moreover, BiP expression is up-regulated by ischemia in both focal and global transient ischemia models (Ito et al., 2001; Shibata et al., 2003; Tajiri et al., 2004).

Using a BiP reporter assay system, we previously identified BiP inducer X (BIX) (Kudo et al., 2008). We thought that agents that activate defense mechanisms against ER stress might have the potential to become new drugs for use against brain ischemia, and so we set out to evaluate the neuroprotective effects of BIX against the cell death induced by ischemia. In the present study, we examined the effects of BIX in a gerbil global transient ischemia model. Intracerebroventricular pretreatment with BIX at 40 μg increased BiP mRNA in the hippocampus, while administration of BIX at 10 and 40 μg protected against the cell death in the hippocampal CA1 subfield induced by transient forebrain ischemia (as revealed by immunohistochemical analysis using NeuN and TUNEL-staining; Figs. 5 and 6). We previously showed that intracerebroventricular administration of BIX at 5 to 20 μg dose-dependently reduced the extent of both cerebral infarction and neuronal cell death after MCA occlusion in mice, particularly in the penumbra region (Kudo et al., 2008). These doses of BIX are roughly equivalent to those given in the present experiments (when expressed per unit body weight). These data indicate that intracerebroventricular administration of BIX protects not only against the apoptosis and/or necrosis induced by MCA occlusion, but also against the delayed neuronal cell death in the hippocampal CA1 subfield induced by global transient ischemia.

If intracerebroventricular volume in mice is approximately 200 μl (Junge et al., 2003), then that in gerbils would be around 600 μl, and the putative concentration of BIX in the cerebral ventricles after intracerebroventricular injection of 40 μg would be approximately 300 μM. Taken together, the above indicates that *in vivo*, the injected BIX probably reaches the brain (the hippocampus at least) at concentrations (5 μM or more) sufficient to exert neuroprotective effects [based on the effective concentrations in our *in vitro* experiments, in which we observed up-regulation of BiP expression (Fig. 2) and neuroprotective effect against tunicamycin-induced cell death in SH-SY5Y cells (Fig. 3)].

What kinds of stress might induce delayed neuronal cell death in the hippocampal CA1 subfield after global ischemia? In our previous study on gerbil transient forebrain ischemia (Oida et al., 2008), we demonstrated that excessive ER stress in the early stage of the ischemia was involved in the execution of cell death in the CA1 subfield. BiP expression in the CA1 subfield was found to be up-regulated at 12 h after global forebrain ischemia in the gerbil, and ATF4 and CHOP were increased in that region (Oida et al., 2008). In a recent study, CHOP mRNA and XBP-1 mRNA showed maximal 14- and 12-fold increases in the hippocampal CA1 following transient global forebrain ischemia plus up to 42 h of reperfusion (Roberts et al., 2007). In the present study, BIX, an inducer of BiP, protected against cell death in the hippocampal CA1 subfield after transient global ischemia. Taken together, the above evidence suggests that ER stress may play a pivotal role in post-ischemic neuronal death in the gerbil hippocampal CA1 subfield, and that the protective effects of BIX against global transient ischemia may result from its BiP-inducting activity.

In conclusion, our results suggest that BIX, a selective inducer of BiP, inhibits the cell death induced by ER stress in SH-SY5Y cells as well as the neuronal cell death in the hippocampal CA1 subfield observed in a gerbil global transient ischemia model. Hence, drugs that selectively induce BiP may activate defense mechanisms against ER stress, resulting in a neuroprotective effect, and such drugs may therefore have potential as new therapeutic interventions against the effects of stroke.

4. Experimental procedures

4.1. *Experimental materials*

1-(3,4-Dihydroxy-phenyl)-2-thiocyanato-ethanone (BIX) was synthesized in our laboratory. Male adult Mongolian gerbils (Kyudo, Fukuoka, Japan), weighing 60–80 g, were used for experiments on transient global forebrain ischemia. The animals were allowed *ad libitum* access to food and water. The present

experiments were performed in accordance with the Guideline for Animal Experiments of the Gifu Pharmaceutical University.

The drugs used and their sources were as follows. Paraformaldehyde (Wako Pure Chemical Industries, Osaka, Japan), sucrose (Wako), sodium hydrogenphosphate 12-water (Nacalai tesque, Kyoto, Japan), sodium dihydrogen phosphate dihydrate (Nacalai tesque), potassium chloride (Wako), sodium chloride (Kishida Chemical, Osaka, Japan), nembutal (Dainippon Pharmaceutical, Osaka, Japan), Triton X-100 (BIO-RAD, Hercules, CA, USA), O.C.T. compound (Sakura Finetechnical, Tokyo, Japan), Vectastain elite ABC kit (Vector Labs, Burlingame, CA, USA), M.O.M. immunodetection kit (Vector Labs), diamino benzidine peroxidase substrate kit (Vector Labs), mouse anti-neuronal nuclei (NeuN) monoclonal antibody (Chemicon, Temecula, CA, USA), mouse anti-BiP/GRP78 antibody (BD Transduction Laboratories, Lexington, KY, USA), mouse anti-β-actin antibody (SIGMA-Aldrich, St. Louis, MO, USA), *In situ* apoptosis detection kit (Takara Shuzo, Otsu, Japan), TSA Biotin system (PerkinElmer Life Sciences Inc., Boston, MA, USA), dimethyl sulfoxide (DMSO; Koso Chemical, Tokyo, Japan), Dulbecco's modified Eagle's medium (DMEM; SIGMA), fetal bovine serum (NSW, Australia), penicillin and streptomycin (Meiji Seika, Tokyo, Japan), tunicamycin (Wako), and thapsigargin (Alexis Biochemicals. Lausen, Switzerland).

4.2. *Cell cultures*

Human neuroblastoma (SH-SY5Y) cells were purchased from the European Collection of Cell Cultures (ECACC) and maintained in DMEM containing 10% FBS, 100 U/ml penicillin, and

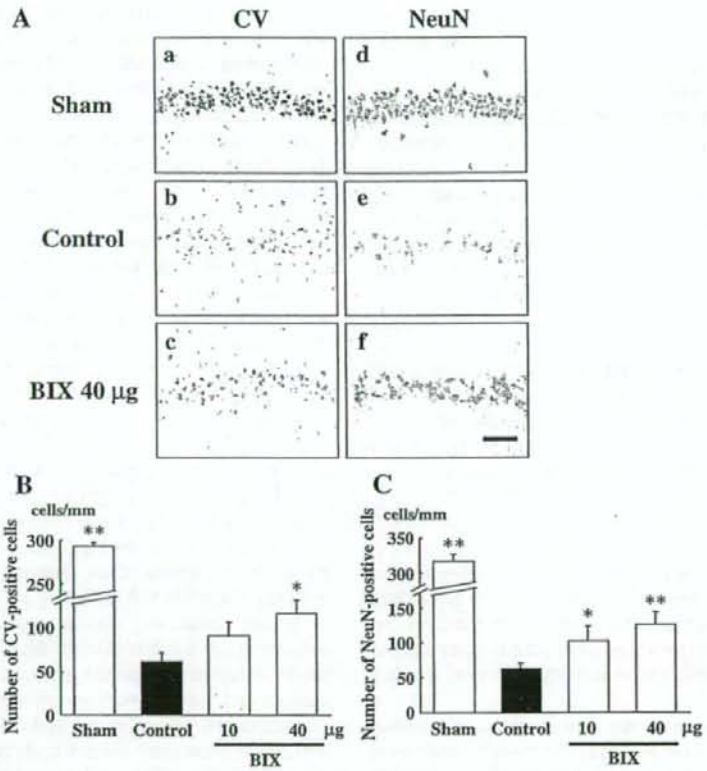

Fig. 5 – Histological analysis of hippocampus after ischemia in gerbil. Under anesthesia, vehicle (10% DMSO in saline) or BIX (10 or 40 μg) was stereotaxically administered into the lateral ventricle. Thirty minutes after the righting reflex had been regained, both common carotid arteries were exposed and occluded bilaterally for 5 min. Brains were analyzed 7 days after ischemia. (A) Representative photomicrographs of cresyl violet (CV)-positive and (NeuN)-positive cells in the hippocampal CA1. In sham-operated animal (Sham), CA1 pyramidal cells were well preserved (a). Vehicle-treated ischemia (Control) group showed marked damage to CA1 pyramidal cells (b). BIX (40 μg) treatment group was protected against the neuronal cell death induced by ischemia (c). Staining, signals for NeuN were well preserved in sham-operated animals (d). In the control group, the number of NeuN-positive cells appeared to be significantly decreased (e), but BIX party prevented the decrease (f). Scale bar=50 μm. (B) Quantitative analysis of CV-positive cells in hippocampal CA1. A decrease in the number of CV-positive neurons in the hippocampal CA1 was detected at 7 days after ischemia. BIX protected against the decrease in a dose-related manner. (C) Quantitative analysis of NeuN-positive cells in hippocampal CA1. A decrease in the number of NeuN-positive neurons in the hippocampal CA1 was detected at 7 days after ischemia. BIX protected against the decrease in a dose-related manner. Values are expressed as the mean and standard error ($n=5$–8). $^{*}p<0.05$, $^{**}p<0.01$ vs. Control.

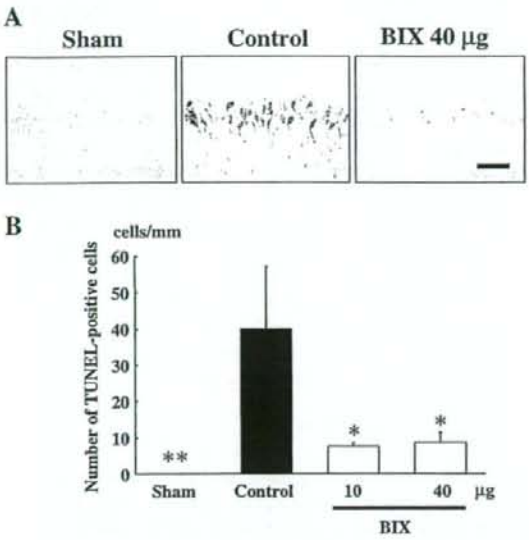

Fig. 6 – Detection of apoptotic cells using TUNEL assay. Under anesthesia, 5 μl of vehicle (10% DMSO in saline) or BIX (10 or 40 μg) was stereotaxically administered into the lateral ventricle. Thirty minutes after the righting reflex had been regained, both common carotid arteries were exposed and occluded bilaterally for 5 min. Brains were analyzed 7 days after ischemia. In the detection of apoptosis, TUNEL signals were not detected in the sham-operated group, while the vehicle-treated ischemia (control) group showed a marked increase. BIX appeared to offer significant protection against this increase in TUNEL-positive cells. Scale bar=50 μm. (B) Quantitative analysis of TUNEL-positive cells in hippocampal CA1. An increase in the number of TUNEL-immunopositive neurons in the hippocampal CA1 was detected at 7 days after ischemia. BIX suppressed the increase at each dose used. Values are expressed as the mean and standard error (n=5–8). *p<0.05, **p<0.01 vs. Control.

100 μg/ml streptomycin in a humidified atmosphere of 5% CO_2 at 37 °C. Cells were passaged by trypsinization every 3–5 days. SH-SY5Y cells were seeded at 1×10^5 cells per well into a 12-well plate, then incubated for 24 h at 37 °C in a humidified atmosphere of 5% CO_2. Thereafter, the entire medium was replaced with fresh medium containing 1% FBS and a given concentration of BIX. Incubation was allowed to proceed for 24 h, and cells were then collected for western blot analysis.

4.3. *Cell-death assay*

SH-SY5Y cells were seeded at 1×10^4 cells per well into a 96-well plate, then incubated for 24 h at 37 °C in a humidified atmosphere of 5% CO_2. BIX at 1 to 5 μM was pre-treated for 24 h, and thereafter the entire medium was replaced with fresh medium containing 1% FBS and the same concentration of BIX together with 2.0 μg/ml tunicamycin. Cell viability and nuclear staining assays were carried out after further 24 h incubation. Cell death was assessed on the basis of combination staining with Hoechst 33342 and YO-PRO-1 (Molecular Probes, Eugene, OR, USA). Hoechst 33342 (λ_{ex}360 nm, λ_{em}>490 nm) freely enters living cells and therefore stains the nuclei of viable cells, as well as those that have suffered apoptosis or necrosis. Apoptotic cells can be distinguished from viable and necrotic cells on the basis of nuclear condensation and fragmentation. YO-PRO-1 (λ_{ex}491 nm, λ_{em}>509 nm) is a membrane-impermeable dye that is generally excluded from viable cells, whereas early-stage apoptotic and necrotic cells are YO-PRO-1 positive. At the end of the culture period, Hoechst 33342 and YO-PRO-1 dyes were added to the culture medium (at 8 and 0.2 μM, respectively) for 15 min. Images were collected using an OLYMPUS IX70 inverted epifluorescence microscope (OLYMPUS, Tokyo, Japan). A total of at least 300 cells per condition were counted in a blind manner by single observer (H.I.).

4.4. *Western blot analysis*

Cells were washed with PBS, harvested, and lysed in RIPA buffer (SIGMA) supplemented with protease inhibitor cocktail (SIGMA) and phosphates inhibitor cocktails 1 and 2 (SIGMA). Lysates were centrifuged at 12,000 ×g for 15 min at 4 °C. Supernatants were collected and boiled for 5 min in SDS sample buffer (Wako). Equal amounts of protein were subjected to 10% SDS-PAGE gel, then transferred to polyvinylidene difluoride membranes. After blocking with Block Ace (Snow Brand Milk Products Co. Ltd, Tokyo, Japan) for 30 min, the membranes were incubated with the primary antibody (anti-BiP/GRP78 antibody or anti β-actin antibody). After this incubation, the membrane was incubated with the secondary antibody [HRP-conjugated goat anti-mouse IgG (Pierce Biotechnology, Rockford, IL, USA)]. The immunoreactive bands were visualized using Super Signal® West Femto Maximum Sensitivity Substrate (Pierce Biotechnology), then measured using GelPro (Media Cybernetics, Silver Spring, MD, USA).

4.5. RT-PCR

SK-N-SH cells, and gerbil brain homogenate and hippocampus were washed with PBS, then collected by centrifugation. Total RNA was isolated from the cells using a RNeasy kit (Qiagen K.K., Tokyo, Japan) according to the manufactures protocol. RNA concentrations were determined spectrophotometrically at 260 nm. First-strand cDNA was synthesized in a 20 μl reaction volume using a random primer (Takara, Shiga, Japan) and Moloney murine leukemia virus reverse transcriptase (Invitrogen, Carlsbad, CA, USA). PCR was performed in a total volume of 30 μl, which contained 0.8 μM of each primer, 0.2 mM dNTPs, 3 U Taq DNA polymerase (Promega), 2.5 mM $MgCl_2$, and 10× PCR buffer. The amplification conditions for semi-quantitative RT-PCR analysis were as follows: an initial denaturation step (95 °C for 5 min), 22 cycles of (95 °C for 1 min, 55 °C for 1 min and 72 °C for 1 min), and a final extension step (72 °C for 7 min). The numbers of amplification cycles for the detection of BiP and β-actin were 18 and 15, respectively. The primers used for amplification were as follows: BiP, 5′-GTTTGCTGAGGAAGACAAAAAGCTC-3′ and 5′-CACTTCCATAGAGTTTGCTGATAATTG-3′; β-actin, 5′-TCCTCCCTGGAGAAGAGCTAC-3′ and 5′-TCCTGCTTGCTGATCCACAT-3′. The PCR products were resolved by electrophoresis through a 4.8% (w/v) poly-acrylamide gel. The